



저작자표시-비영리-변경금지 2.0 대한민국

이용자는 아래의 조건을 따르는 경우에 한하여 자유롭게

- 이 저작물을 복제, 배포, 전송, 전시, 공연 및 방송할 수 있습니다.

다음과 같은 조건을 따라야 합니다:



저작자표시. 귀하는 원저작자를 표시하여야 합니다.



비영리. 귀하는 이 저작물을 영리 목적으로 이용할 수 없습니다.



변경금지. 귀하는 이 저작물을 개작, 변형 또는 가공할 수 없습니다.

- 귀하는, 이 저작물의 재이용이나 배포의 경우, 이 저작물에 적용된 이용허락조건을 명확하게 나타내어야 합니다.
- 저작권자로부터 별도의 허가를 받으면 이러한 조건들은 적용되지 않습니다.

저작권법에 따른 이용자의 권리는 위의 내용에 의하여 영향을 받지 않습니다.

이것은 [이용허락규약\(Legal Code\)](#)을 이해하기 쉽게 요약한 것입니다.

[Disclaimer](#)

February 2020
Master's Degree Thesis

5G microstrip patch array antenna using corporate-series-feed network

Graduate School of Chosun University
Department of Information and Communication
Engineering

Janam Maharjan

5G microstrip patch array antenna using corporate-series-feed network

February 25, 2020

Graduate School of Chosun University
Department of Information and Communication
Engineering

Janam Maharjan

5G microstrip patch array antenna using corporate-series-feed network

Advisor: Prof. Dong-You Choi

A thesis submitted in partial fulfillment of the
requirements for a master's degree in engineering

October 2019

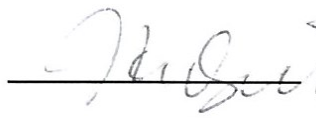

Graduate School of Chosun University
Department of Information and Communication
Engineering

Janam Maharjan

This is to certify that the master's thesis of
Janam Maharjan
has been approved by examining committee for the
thesis requirement for the master's degree in
Engineering.

Committee Chairperson

Prof. Seung-Jo Han


_____ 

Committee Member

Prof. Jae-Young Pyun


_____ 

Committee Member

Prof. Dong-You Choi


_____ 

November 2019

Graduate School of Chosun University

Table of contents

List of figures	iii
List of tables	vii
Abstract	viii
요약	xi
1. Introduction	1
1.1 Overview.....	1
1.2 Objectives	5
1.3 Contributions	6
1.4 Thesis layout	7
2. Theory and background	8
2.1 5G technology.....	8
2.2 Microstrip patch antenna	11
2.2.1 Designing a rectangular microstrip patch.....	13
2.3 Antenna parameters	15
2.3.1 Return loss.....	15
2.3.2 Voltage standing wave ratio (VSWR).....	16
2.3.3 Radiation efficiency	17
2.3.4 Radiation pattern	17

2.3.5	Antenna gain	18
3.	Modeling of proposed antennas, simulations and results	19
3.1	Single element.....	19
3.1.1	Single patch element design.....	19
3.1.2	Comparision of single patch element results.....	21
3.2	Array antenna with series feed network	26
3.2.1	Series-fed array antenna design.....	26
3.2.2	Comparision of series-fed array antenna results	27
3.3	Array antenna with corporate feed network	33
3.3.1	Corporate-fed array antenna design	33
3.3.2	Comparision of corporate-fed array antenna results	35
3.4	Proposed array antenna with corporate-series feed network	40
3.4.1	Corporate-series-fed array antenna design	40
3.4.2	Comparision of simulated and mesured results.....	42
3.5	Corporate-series-fed array antenna on FR4 substrate.....	49
3.5.1	Design of array antenna on FR4 substrate	49
3.5.2	Comparision of results between FR4 and Taconic.....	52
4.	Conclusion	55
	Acknowledgement	57
	References	58

List of figures

Figure 1-1. Air attenuation at different frequency bands	3
Figure 2-1. Geometry of conventional microstrip antenna.....	13
Figure 3-1. Geometry of single patch element (a) without Yagi elements, (b) with Yagi elements	20
Figure 3-2. S_{11} plot of single patch element with and without Yagi elements	22
Figure 3-3. VSWR of single patch element with and without Yagi elements	22
Figure 3-4. Radiation patter of single patch element with Yagi elements (a) at 26.4GHz, (b) at 28GHz, and (c) at 29.4GHz	23
Figure 3-5. Radiation efficiency of single patch element with and without Yagi elements	24
Figure 3-6. Peak realized gain of single patch element with and without Yagi elements	24
Figure 3-7. Geometry of series-fed microstrip array antenna	27
Figure 3-8. S_{11} of series-fed microstrip array antenna with stub lengths 2.2mm, 3.2mm, 4.2mm, and 5.2mm.....	28
Figure 3-9. VSWR of series-fed microstrip array antenna (with stub length 3.2mm).....	29

Figure 3-10. Radiation pattern of series-fed microstrip array antenna (a) at 26.4GHz, (b) at 28GHz, and (c) at 29.4GHz	30
Figure 3-11. Radiation efficiency of series-fed microstrip array antenna	31
Figure 3-12. Peak realized gain of series-fed microstrip array antenna	31
Figure 3-13. Geometry of corporate-fed microstrip array antenna	34
Figure 3-14. S_{11} of corporate-fed microstrip array antenna with feed lengths 4.75mm, 5.3mm, and 5.85mm.	36
Figure 3-15. VSWR of corporate-fed microstrip array antenna (with feed length 4.75mm).....	36
Figure 3-16. Radiation pattern of corporate-fed microstrip array antenna (a) at 26.7GHz, (b) at 28GHz, and (c) at 29.7GHz.....	37
Figure 3-17. Radiation efficiency of corporate-fed microstrip array antenna	38
Figure 3-18. Peak realized gain of corporate-fed microstrip array antenna	38
Figure 3-19. Geometry of proposed corporate-series-fed microstrip array antenna.....	41
Figure 3-20. Fabricated prototype of proposed corporate-series-fed microstrip array antenna (a) top view, (b) bottom view .	41

Figure 3-21. Measured and simulated S_{11} of proposed corporate-series-fed microstrip array antenna vs S_{11} of series- and corporate-fed array antennas 43

Figure 3-22. Measured and simulated VSWR of proposed corporate-series-fed microstrip array antenna..... 43

Figure 3-23. Radiation efficiency of proposed corporate-series-fed microstrip array antenna 44

Figure 3-24. Peak realized gain of proposed corporate-series-fed microstrip array antenna vs peak realized gain of series- and corporate-fed array antennas 44

Figure 3-25. Radiation pattern of the proposed corporate-series-fed array antenna at 27GHz, 28GHz, and 29GHz 46

Figure 3-26. Geometry of single patch element on FR4 substrate 49

Figure 3-27. Geometry of corporate-series-fed microstrip array antenna on FR4 substrate 51

Figure 3-28. Fabricated prototype of corporate-series-fed microstrip array antenna on FR4 substrate (a) top view, (b) bottom view..... 51

Figure 3-29. Measured and simulated S_{11} of corporate-series-fed microstrip array antennas on Taconic substrate vs on FR4 substrate 53

Figure 3-30. Radiation efficiencies of corporate-series-fed microstrip array antennas on Taconic substrate vs on FR4 substrate 53

List of tables

Table 1. Dimensions of the single patch element	21
Table 2. Dimensions of the series-fed microstrip array antenna	27
Table 3. Dimensions of the corporate-fed microstrip array antenna .	35
Table 4. Dimensions of the proposed microstrip array antenna	42
Table 5. Comparison between array antenna models	47
Table 6. Dimensions of the single patch in FR4 substrate.....	50
Table 7. Dimensions of the array antenna on FR4 substrate	52

Abstract

5G microstrip patch array antenna using corporate-series-feed network

Janam Maharjan

Advisor: Prof. Dong-You Choi, Ph.D.

Department of Information and

Communication Engineering

Graduate School of Chosun University

Technology has become an essential part of human life and in today's world; technology poses many new challenges, as it keeps on getting better, smarter and faster. Fourth generation (4G) mobile communication has been deployed in many countries and now the world is looking on to 5th generation (5G) for the future. Moreover, it is believed that 5G communication will bring larger bandwidth and coverage, faster speed, high data rate, and huge device density, meeting the current demands of the wireless technology. One of the basic part of a communication system is its antenna, and to develop a system working on 5G, an antenna suitable for 5G application should be designed first. The proposed work in this thesis presents microstrip patch array antenna producing wide bandwidth with operating frequency band at 28GHz, suitable for 5G application.

A simple microstrip patch array antenna with a corporate-series feed network is designed and presented for 5G applications. The array uses the elements of a rectangular microstrip patch with two insets and two

slots on both sides, three director elements on top, and two reflector elements on each side of the patch. First, series- and corporate-fed array antennas are designed and tested separately. In array antenna with series feed network, director elements are placed only on top of the top most patch, while the reflector elements are placed only below the patch connected to the feedline. In array antenna with corporate feed network, director elements are placed above every patch, while only one reflector element is placed on the lower open side of the patch. Both antennas operate in the frequency band around 28GHz, with wide bandwidth of 25.67~30.34GHz and 24.85~30.32GHz respectively. Series-fed array antenna has highest peak gain of 7.98 dB at 29.3GHz. Similarly, corporate-fed array antenna has highest peak gain of 8.8 dB at 26.7GHz. In the final proposed design, both series and corporate feeding techniques are combined to obtain a corporate-series-fed array antenna. Yagi elements are also placed in similar manner as in series- and corporate-fed array antennas.

Finally, microstrip patch array antenna with a corporate-series feed network, suitable for 5G application, is compared with series- and corporate-fed array antennas. The results indicate that the proposed array antenna achieved a wide operating frequency bandwidth of 25.04~30.87GHz. In addition, proposed array antenna's gain over the operating frequency band is higher; achieving highest peak gain of 9.49 dB at 26GHz. Addition of Yagi elements improved the gain throughout the frequency band.

The antennas are designed using two different substrates: Taconic and FR4. Both substrates are easily available. Based on the performance of the antennas, the final proposed antenna is built on Taconic substrate. The antennas are designed using finite element method based High Frequency Structure Simulator (HFSS) and their performances are analyzed on the basis of the reflection coefficient, VSWR, radiation patterns, antenna efficiency and antenna gain.

요약

직.병렬 급전 네트워크를 활용한 5G 마이크로 스트립 패치 배열 안테나

Janam Maharjan

Advisor: Prof. Dong-You Choi, Ph.D.
Department of Information and
Communication Engineering,
Graduate School of Chosun University

최근 이동통신 기술은 점점 더 스마트 해지고 빨라지면서 우리들의 삶속에서 필수적인 부분이 되었다. 많은 국가에서 4 세대 (4G) 이동통신을 활용하고 있으며, 보다 나은 미래를 위하여 5 세대 (5G) 이동통신에 대해 활발히 연구하고 있다. 특히, 5G 통신은 초고속, 초연결, 저지연 고신뢰성이라는 현재 무선통신의 요구를 충족시킬 것으로 판단된다. 5G 이동통신과 이를 응용하기 위하여 5G 안테나를 설계해야 하며, 본 논문에서는 5G 애플리케이션에 적합한 28GHz 주파수 대역의 마이크로스트립 패치 배열 안테나를 제안하였다.

본 논문에서 5G 애플리케이션을 위하여 제안한 4소자 마이크로스트립 패치 배열 안테나는 양쪽에 2 개의 삽입구와 2 개의 슬롯, 상단에 3 개의 도파기 및

패치의 각 측면에 반사기를 추가하였다. 직렬 및 병렬 급전 배열 안테나를 각각 설계하고 시뮬레이션을 수행하였으며, 직렬 급전 배열 안테나에서 도파기는 최상위 패치 위에만 배치하고 반사기는 피드 라인에 연결된 패치 아래에만 배치하였다. 병렬 급전 배열 안테나에서는 도파기를 모든 패치 위에 배치하고 반사기는 패치 아래에만 배치하였다. 두 안테나는 각각 28.67~30.34GHz 및 24.85~30.32GHz 주파수 대역에서 활용할 수 있다. 직렬 급전 배열 안테나는 29.3GHz 에서 7.98dB 의 최고 이득을 가지며, 병렬 급전 배열 안테나는 26.7GHz 에서 8.8 dB 의 최고 이득을 갖는다. 최종적으로 직렬 급전 방식과 병렬 급전 방식을 결합하였으며, Yagi 요소는 직렬 및 병렬 급전 배열 안테나와 유사한 방식으로 배치하였다.

제안한 직·병렬 급전 네트워크를 활용한 마이크로스트립 패치 배열 안테나를 직렬 및 병렬 급전 배열 안테나와 비교한 결과, 제안한 배열 안테나가 25.04~30.87GHz 의 주파수 대역에서 동작함을 확인할 수 있었으며, 제안한 배열 안테나의 이득은 동작 주파수 대역 내 26GHz 에서 9.49 dB 의 최고 이득을 갖고, Yagi 요소를 추가함으로써 이득이 향상됨을 확인할 수 있었다.

제안한 안테나는 유한 요소 방법 기반 고주파 구조 시뮬레이터 (HFSS)를 사용하여 설계되었으며, 반사계수, VSWR, 방사패턴, 안테나 효율 및 안테나 이득 등의 시뮬레이션 결과를 바탕으로 비교적 가격이 저렴하고 쉽게 구할 수 있는 Taconic 과 FR4 기판을 사용하여 제작하였다.

1. Introduction

1.1 Overview

Over the course of years, momentous progressions in the field of communication networks has been put forward with the incredible growth in the productions, usages as well as research of wireless devices. This has made evolution in the field of communication networks inevitable in the near future. The latest 4th generation (4G) LTE has been able to dominate the market by efficiently combining various commercial services. The technology has improved the quality in the user's end by meeting the demands of high-throughput, high data rates, and high-speed connectivity. However, with the recent implementation of the 4th generation (4G) of mobile communication in many countries, the world is now shifting the focus to 5th generation (5G) for the future. Owing to the growth in mobile technology across the world and user demands for wireless devices and applications, such as internet of things (IoTs) that require higher bandwidths has led to a global bandwidth shortage for current wireless cellular networks. 4G is a huge upgrade, but the technology faces bandwidth inadequacy, which still limits the obligatory advancements, while consuming limited bandwidth spectrum <3GHz. The 5G communication system is the answer to these new demands; this technology will offer a larger spectrum and coverage, energy efficiency, high data rate (10–50 Gbps), and the device density that it will support will be higher than that supported by current 4G systems.

The 5G system shall exploit millimeter-wave bands [1] from the available spectrum to accomplish the future demands of high capacity, throughput [2, 3] and further improve the communication experience. The main reason for 5G

to use millimeter-wave bands is the massive amount of frequency bandwidth it has in disposal [4]. The millimeter-wave band is the slice of the electromagnetic spectrum ranging from 30GHz to 300GHz with wavelengths from 10mm to 1mm. Though the millimeter-wave band frequencies are attracting great attention at present, in the past, they were mostly applied in the field of defense and radio astronomy applications due to their high application cost and limited devices working at those frequencies. However, the advancement in the field of technology now sees rapid growth in millimeter-wave band applications, as they play a huge role in the development of low power, highly integrated, low cost wireless systems [5]. For 5G, the Third Generation Partnership Project (3GPP) has allocated the spectrum in two different frequency ranges. Frequency range 1 includes frequency bands below 6GHz, and frequency range 2 includes frequency bands above 24GHz and into the millimeter-wave range (24, 26, 28, and 39GHz) [6].

Microstrip patch antennas have been preferred for antenna design because their characteristics are suitable for commercial wireless applications. They are smaller, lightweight, and easy to fabricate; they can have different shapes, such as rectangular, square, and triangular, and they support high-density packaging. The manufacturing cost is also low. Microstrip patch antennas support various feed techniques and can be developed into arrays to improve the gain and achieve the desired pattern requirements. Owing to these reasons, microstrip patch antennas have proven to be a strong candidate for millimeter-wave applications. Thus, 5G antennas have been developed using the microstrip patch technology. For better results, microstrip array antennas have also been employed and researched for 5G applications [7–11]. The major limitations of using microstrip patch antennas are lower gain and bandwidth.

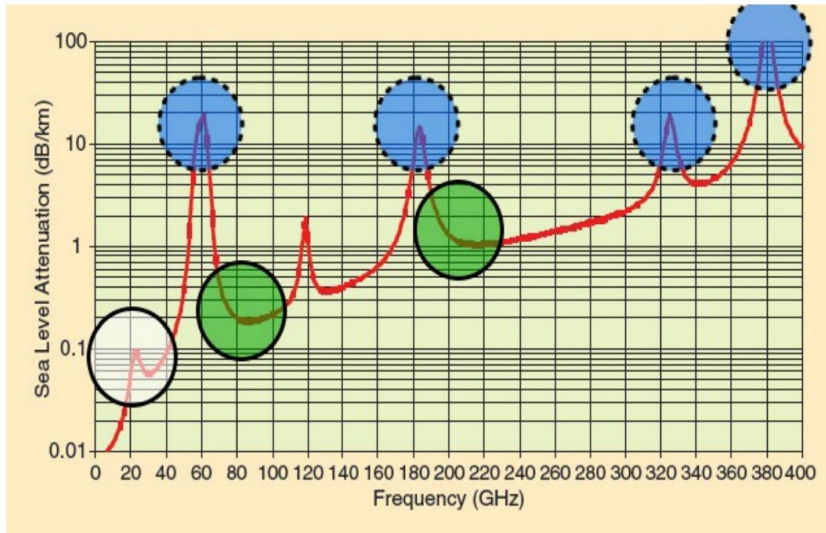


Figure 1-1. Air attenuation at different frequency bands [15]

Although millimeter waves are the future of wireless communication, they have a few flaws. One of them is the significant free-space path loss caused by the high operating frequency bands [12]. Millimeter waves are also susceptible to high propagation loss because of atmospheric absorption. Thus, the loss factor that reduces the gain of the antenna must be considered while designing a system for 5G communication [13]. However, the band of frequencies below 28GHz has relatively less attenuations. Local Multipoint Distribution Service (LMDS) broadband spectrum that exists below 28GHz are underutilized, and have lower atmospheric absorptions similar to free space path loss of 1GHz to 2GHz cellular bands. They are also less affected compared to millimeter wave bands above 30GHz, as rain attenuation and oxygen loss does not increase significantly at 28GHz. Compared to the current networks, they may even offer better conditions for propagation when the availability of adaptive antennas with high gain and cell sizes in order of 200 meters are considered. [14, 15] has presented the data analysis of various frequency bands and effects

of sea level attenuation on them. As seen from the Fig. 1-1, taken from the research, it is clear that the atmospheric absorption drops down at 28GHz (denoted by white circle), i.e. 0.06 dB/km, which is almost negligible.

The easy feeding techniques are few of the useful characteristics of microstrip patch antennas in wireless applications. The microstrip patch elements of an array antenna can be fed using a single line or multiple lines, depending on the requirement of the system. Generally, there are two types of array feeding structures, namely parallel-fed, also known as corporate-fed, and series-fed. In few cases, series and parallel feeding techniques are combined to form corporate-series-fed network [16]. In corporate feed network, several power dividers comprising numerous discontinuities and long transmission lines are used, which cause spurious radiation and substantial dielectric loss to occur, while conversely, the series feed network utilizes short transmission lines enhancing antenna efficiency [17].

A network using series feeding technique is a type of feed network that consists of a continuous transmission line through which a proportion of energy is progressively coupled into each element of an array along the line. In [18], a series feed technique has been employed to feed a 4×4 planar microstrip array antenna with a modular structure and small dimension that can operate in 5G network at 28GHz. In [19], a modified 3×3 series-fed patch array antenna capable of beam steering is presented for 28GHz millimeter-wave applications. Corporate feed is a popular feed technique used for microstrip array antennas. In the case of corporate feed network, the power is equally split at each junction of the microstrip patch array antenna for uniform distribution. In [20], a 16-element microstrip patch array antenna suitable for 5G application is designed with a corporate feeding technique and is employed

to achieve a bandwidth greater than 300MHz. Some researchers have combined the series and corporate feed techniques to achieve the desired antenna outputs. In [21], a rectangular microstrip patch array antenna with a 16-element corporate–series feed network is proposed; it operates at 28GHz for 5G applications. However, the antennas mentioned above individually achieved comparatively narrow bandwidths with series feed or corporate feed networks.

Finally, 5G communication requires high gain. Various methods have been applied on microstrip patch antennas to improve gain while also maintaining wide bandwidth. Among those techniques, application of Yagi elements is also widely famous due to its simple structure and high gain [22]. Use of Yagi elements in microstrip patch antenna have many benefits over other commonly used antenna techniques for communication systems [23]. Thus, a microstrip patch array antenna with corporate-series feed network and Yagi elements, capable of achieving wide bandwidth and high gain, could be considered.

1.2 Objectives

As 4G is being implemented around the world, 5G communication is the future of the technology. To build the communication system for 5G, the basic component of the wireless system, antenna, should be designed first. Various researches are being conducted to build antenna capable for 5G applications. The main purpose of this thesis is to propose an antenna system that can support 5G communication. Considering the discussions discussed in above section, the goals and ideas for this research are set, which are as follows:

- To design a simple microstrip array antenna operating at 28GHz frequency band with a corporate–series feed network and Yagi elements to achieve a wide bandwidth and high gain.
- Prior to designing the corporate–series-fed array antenna,
 - Design a single patch element operating at 28GHz frequency
 - Employ patch elements in series-fed and corporate-fed array antennas separately.
- To compare the proposed corporate–series-fed array antenna with series-fed and corporate-fed array antennas.
- To use easily available and affordable substrate material for the proposed array antenna.

1.3 Contributions

In this thesis, the design of the microstrip patch array antenna with corporate-series feed network for 5G has been presented. At first, a single-element microstrip patch antenna is designed and then transformed into array using series-fed and corporate-fed networks separately. Later, the feeding techniques are combined to form corporate-series feed network. Using corporate-series feed network along with Yagi elements, the proposed microstrip-patch array antenna for 5G communication is designed. All arrays are simulated using the Ansoft High-Frequency Structure Simulator (HFSS), which is a commercial electromagnetic simulator. The array antennas are then compared with each other. The results of the comparisons show that the array antenna with combined corporate and series feed network performs better than array antenna with only series or corporate feed network for 5G. Addition of Yagi elements also improved the overall gain and widened the bandwidth of the antenna. The final proposed antenna is corporate-series fed microstrip patch array, with

Yagi elements. The antenna is also manufactured and the measurements are taken in real environment.

1.4 Thesis layout

Rest of the thesis is organized as follows:

Section 2 provides the basic theory and background overview of the 5G communication, followed by various potential technologies that can be applied to make 5G communication possible. Further, general idea of the microstrip patch antennas, their advantages and disadvantages are discussed. Brief explanation of antenna parameters are also given in this chapter.

In section 3, detailed information regarding the designing of the proposed microstrip patch array antenna with corporate-series feed network is presented. Prior to that, design procedure of single patch element, followed by the construction of series-fed and corporate-fed array antennas are explained. The simulation results of individual antennas are also presented. In the end, series-fed, corporate-fed and the proposed corporate-series fed microstrip patch array antennas are compared. Comparisons are also made between proposed designs built on FR4 substrate and Taconic substrate. For this, a complete analysis on simulated and measured results are presented and compared based on reflection coefficient, VSWR, radiation patterns, antenna efficiency, and antenna gain.

Finally, the last section presents the conclusion drawn from the current study and future possibilities.

2. Theory and background

2.1 5G technology

5G or also known as the 5th generation wireless systems is a term used as the next main phase of telecommunications standards beyond the current 4G [24]. It is well known that with the rapid increase in use of wireless technology around the world, there has been dramatic traffic growth over few years, with increasing demands of greater bandwidth, larger network capacity, and faster data speed. These demands are expected to be fulfilled by the introduction of 5G. 5G communication is assumed to achieve higher capacity and higher data rates compared to 4G networks. 5G technology is considered as the next step in the field of communication, which will offer wider bandwidths, reliable user experience, faster speed, massive device capacity and more.

The current 4G communication network has tried adopting various technologies, such as massive multiple-input multiple-output (M-MIMO), beamforming, device-to-device (D2D) communications, and small cell deployment, to provide seamless services to the devices and users requiring wireless network. As 5G is probable to adopt the modified version of similar technologies, the current wireless devices working on 4G should also support the new 5G. Thus, to develop 5G systems, following technologies have been listed as the potential technologies for 5G: small cell deployment, utilization of millimeter-wave band, M-MIMO and beamforming.

Deploying smaller cells in large numbers in limited space to improve signal power and offload macrocells is the target of dense small cell deployment. Small cells can offer cost effective solution to improve the network capacity. They can be deployed indoors as well as outdoors within a limited cell radius

in larger number, which can result in massive growth of mobile traffic. This happens as small cells can reuse the spectrum within a limited space. Due to these benefits, dense small cell deployment can play a vital role to accomplish the objective of 5G. However, it has its own limitations. Since the coverage area of cell is small, there will be significant increase in handoff rate. In addition, since small cell becomes denser and multiple small cells will have to be deployed in limited space, inter-cell interference might occur.

Due to favorable propagation characteristics, most of the communication systems have been functioning in the microwave band under 3GHz. With the rapid increase in use of wireless devices, microwave band is being overloaded, increasing the demand of more frequency bands. By utilizing millimeter-wave band, 5G can address the bandwidth demand. Since millimeter-wave band have substantial available bandwidth, 5G networks can use the higher spectrum to satisfy bandwidth scarcity. US Federal Communications Commission (FCC) has listed the promising millimeter-wave band for future 5G systems, which includes local multipoint distribution service (LMDS) band from 28~30GHz, license free band at 60GHz, bands from 71~76GHz, 81~86GHz, and 92~95GHz in the E-band [25]. Thus, millimeter wave bands from 20~90GHz is expected to be used by 5G systems.

Though millimeter-wave band is a boon to 5G system, it has few limitations. One of the limitations is that to minimize high path loss, millimeter-wave band must be used within a cell radius less than 100m. Signal attenuation at higher frequency bands is another major challenge faced by millimeter-wave band. Oxygen and water vapor absorbs the energy radiated by millimeter-wave causing signal attenuation. Millimeter-wave signals also have very high losses when penetrating through solid materials. These are few challenges that needs

to be addressed properly to utilize millimeter-wave band for 5G applications. In this thesis, an array antenna operating around 28GHz band is designed. The frequency band is less affected by atmospheric attenuation.

Massive MIMO and beamforming are other potential technologies that could aid 5G communication. M-MIMO deals with large number of antennas organized at one point. Thus, M-MIMO is deployed at base stations equipped with numerous antennas to accommodate many co-channel users at a time. Beamforming is focusing of power at certain point and direction with narrower beam width but large gain. With the deployment of M-MIMO along with beamforming technique, significant improvement in signal strength could be attained, further resulting in higher cell throughput and better network performance than 4G [26]. Like other technologies for 5G systems, M-MIMO also has few limitations. As the name suggests, massive MIMO uses massive number of antennas. Due to the quantity of antennas used, accurate channel estimation becomes a challenge. In addition, the size of M-MIMO might be another challenge as the requirement of large-sized towers might create technical issues [27]. Thus, while designing the M-MIMO system for 5G, the technical challenges must be addressed.

2.2 Microstrip patch antenna

While the microstrip patch antennas have gained huge popularity in almost every sectors of wireless communication these days due to its many advantages, its origin dates back few twenty to fifty years ago. Though many authors have been credited for the discovery of microstrip antennas, Deschamps first introduced it at the third United States Air Force (USAF) Symposium on Antennas [28] in 1953. However, the antenna took a serious advancement only since the mid 1970's as the development of printed-circuit technology commenced. Since then, the microstrip antennas have been immensely researched and utilized by researches and engineers throughout the world. It has been used for communication purposes in personal systems, mobile satellite, wireless networks, intelligent vehicle highway systems, military applications, and many more. All this due to its following advantages compared with other microwave antenna types: [29–31]

- Microstrip antennas are smaller size, have lower weight and thinner profile configuration.
- They are very easy to design and fabricate.
- They are very conformable, as they can easily fit into a curved surface of a vehicle or product.
- An array of microstrip antennas can be used to form a pattern that is difficult to synthesize using a single element.
- The total cost of designing and fabrication is low.
- Numerous antenna designs can readily produce linear or circular polarization.
- Microstrip antennas can easily achieve dual frequency and dual polarization.

- They can be easily integrated with microwave integrated circuits.
- By combining phase shifters or PIN-diode switches with microstrip antennas, smart antennas can be designed.

Similarly, microstrip antennas also have few limitations, which are as follows: [29–31]

- Microstrip antennas usually produce narrow bandwidth (1%), while mobiles need wider bandwidth (8%).
- They also have lower gain (~6 dB).
- The antenna efficiency is poor.
- Microstrip antennas are very sensitive to environmental factors such as humidity and temperature.
- A microstrip array antenna is affected due to presence of feed network, which decreases the antenna efficiency.

Conventional microstrip antennas consists of three sections: substrate, patch and ground. A substrate is a dielectric layer sandwiched between two conducting layers parallel to each other. The upper conducting layer is called patch and is the main source of radiation. When the power is supplied to the microstrip antennas, the electromagnetic energy fringes off the edges of patch and into the substrate. Patch is usually a thin conductor that is fraction of wavelength in extent ($0.25\lambda_0 - 1\lambda_0$), and is parallel to the lower conducting layer. The lower conducting layer is the ground plane. It reflects the energy back into the free space through the substrate. Both patch and ground are usually etched on the non-magnetic dielectric substrate (opposite to each other). The geometry of the conventional microstrip antenna is shown in Fig. 2-1.

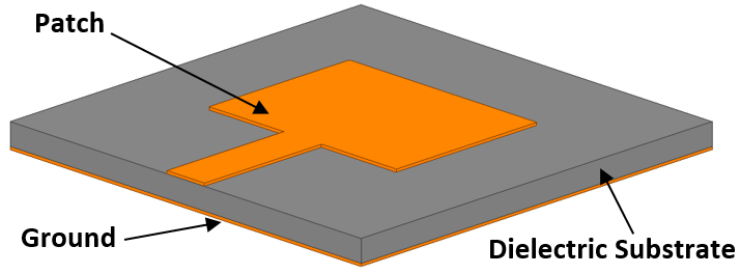


Figure 2-1. Geometry of conventional microstrip antenna

There are numerous designs for patches of microstrip antennas found in the market. However, the most practical ones are rectangular, square, circular or the modified versions of them. Rectangular and square patches are the most common microstrip antennas, as they are easy to analyze, modify and fabricate. Due to the ease of design, the single element of the proposed microstrip array antenna in this thesis is also of rectangular shape.

2.2.1 Designing a rectangular microstrip patch

Since single element of the proposed microstrip patch array antenna of this thesis is a rectangular patch, this section will present the method to design the rectangular microstrip patch. First, to design a patch, the substrate material with thickness h , dielectric permittivity ϵ_r and the target center frequency f_r (resonant) must be chosen. After that, the length L and width W of the rectangular patch can be calculated by the following steps [32]:

Step 1: For efficient radiator, the width W for the patch can be calculated as:

$$W = \frac{c}{2f_r} \sqrt{\frac{2}{\epsilon_r + 1}}, \quad (2.1)$$

where c is the free space light velocity.

Step 2: The effective dielectric constant ϵ_{ff} is determined as:

$$\epsilon_{ff} = \frac{\epsilon_r + 1}{2} + \frac{\epsilon_r - 1}{\sqrt{1 + 12 \frac{h}{W}}}. \quad (2.2)$$

Step 3: Incremental length ΔL generated by fringing fields is determined as:

$$\Delta L = 0.412h \frac{(\epsilon_{ff} + 0.3) \left(\frac{W}{h} + 0.264 \right)}{(\epsilon_{ff} - 0.258) \left(\frac{W}{h} + 0.8 \right)}. \quad (2.3)$$

Step 4: The effective length L_{eff} is determined by equation (2.4) and finally actual length L of the patch is calculated using equation (2.5) as:

$$L_{eff} = \frac{c}{2f_r \sqrt{\epsilon_{ff}}}, \quad (2.4)$$

and

$$L = L_{eff} - 2\Delta L. \quad (2.5)$$

Using the above equations, length L and width W of the patch can be determined for center frequency. The antenna can then be designed using the calculated parameters, and simulated using any simulation tool like HFSS. Its parameters can be further optimized to get the optimum antenna performance.

2.3 Antenna parameters

When designing an antenna, the important factors that make the difference during the design procedure are its parameters. It is important to understand the basic antenna principles in order to understand the performance of the antenna and to select the best antenna for various applications [33]. 5G communication system is the future of wireless technology and antenna is the basic element of that system. Every antennas follow numerous parameters to present its characteristics, and among them, the basic ones for any antenna are radiation pattern, gain, and VSWR. The parameters to determine the characteristics of the proposed microstrip patch array antenna with corporate-series feed are reviewed in this section.

2.3.1 Return loss

Return loss is one of the important antenna parameters to determine the operating bandwidth of the antenna. It is proportional to the square of reflection coefficient (also diagonal S parameter, i.e. S_{11}). Reflection coefficient, denoted by Γ , is the ratio of transmitted to reflected voltage [34]. An antenna with well-matched input transmission should have less than 10% of incident signal loss due to reflection. That is, for an antenna to operate, the return loss of the antenna around the frequency bandwidth should be less than -10 dB. The return loss can be calculated using the following equation:

$$\text{Return Loss} = -10\log|S_{11}|^2 \text{ or, } -10\log|\Gamma|^2 = -20\log|\Gamma|. \quad (2.6)$$

2.3.2 Voltage standing wave ratio (VSWR)

The voltage standing wave ratio (VSWR) is one the basic parameters for designing the antenna. VSWR directly relates to the performance of the antenna, and it is used to portray antenna's efficiency. It can be described as the ratio between the maximum to minimum amplitudes of standing waves [33]. VSWR can be calculated by measuring the voltage along the transmission line leading to an antenna. The equation of VSWR is as follows:

$$VSWR = \frac{V_{max}}{V_{min}} = \frac{1 + |\Gamma|}{1 - |\Gamma|}, \quad (2.7)$$

where

$$\Gamma = \frac{Z_{in} - Z_0}{Z_{in} + Z_0}. \quad (2.8)$$

Z_{in} is the input impedance of the antenna, and Z_0 is the characteristic impedance of the transmission line. Though return loss is widely used in the research field of microwave communication, VSWR is more preferred. For an antenna to operate in certain bandwidth, it should have VSWR of 2:1 or less.

The bandwidth of an antenna is the frequency region in which the antenna operates. It can be simply described as the range of frequencies where all the antenna characteristics (such as radiation efficiency, input impedance, gain, polarization) are within the acceptable values [33]. It is one of the fundamental antenna parameters and is determined by VSWR. The frequency range in which the value of VSWR is 2:1 or less, is the region in which antenna can radiate or receive energy. The range between the upper and lower frequencies of that region is the bandwidth of the antenna. For example, if the frequency range where VSWR is 2:1 or less is 25~30GHz, then the bandwidth is 5GHz.

2.3.3 Radiation efficiency

Radiation efficiency is the ratio of the total power radiated by the antenna to the total power accepted by the antenna at its input terminal during radiation [33]. It is less commonly used to show antenna performance than the basic antenna parameters, but is highly related to VSWR. The total efficiency of the antenna can be calculated as the product of the antenna's radiation efficiency and mismatch loss. It is given as,

Total antenna efficiency = radiation efficiency \times mismatch loss [35]

$$e = \frac{P_r}{P_{in}} = \frac{P_r}{P_r + P_0}, \quad (2.9)$$

where

P_r = Power radiated,

P_0 = Power dissipated in ohmic losses on the antenna,

P_{in} = input power (power accepted by the antenna).

2.3.4 Radiation pattern

The radiation pattern of an antenna can be defined as a mathematical function or graphical representation of the radiation properties of the antenna as a function of space coordinates [36]. Radiation patterns are presented as function of directional coordinates and are usually determined in the far field region. They generally represent antenna properties such as directivity, gain, radiation intensity, power flux density, field strength, phase or polarization [33].

Radiation patterns can be of either three-dimensional or two-dimensional plots. In this thesis, two-dimensional representation of radiation patterns are done to show the performance of the proposed antenna. This is done by presenting two important measurements for the radiation pattern, E-plane and H-plane patterns. E-plane is the plane that contains the direction of electric field (E-field) vector of the radiation from antenna. H-plane contains the direction of magnetic field (H-field) vector radiation, and it is orthogonal to E-plane.

2.3.5 Antenna gain

Antenna gain is a basic parameter to describe the performance of the antenna that is closely related to directivity through radiation efficiency. The difference between gain and directivity is the value of the power used. Antenna gain describes the antenna's ability to concentrate energy in directive beam [37]. It can be further defined as “the ratio of intensity in a given direction to the radiation intensity that would be obtained if the power accepted by an antenna were radiated isotropically [33].” Antenna gain (G) can be expressed in terms of radiation efficiency (e_r) and directivity (D) as:

$$G = e_r D. \quad (2.10)$$

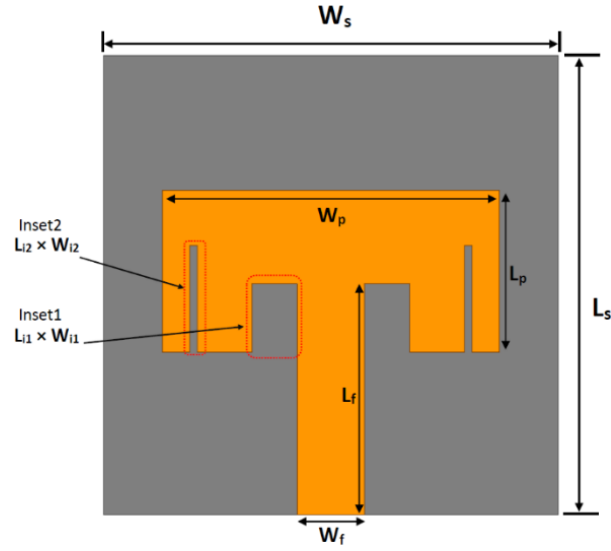
3. Modeling of proposed antennas, simulations and results

3.1 Single element

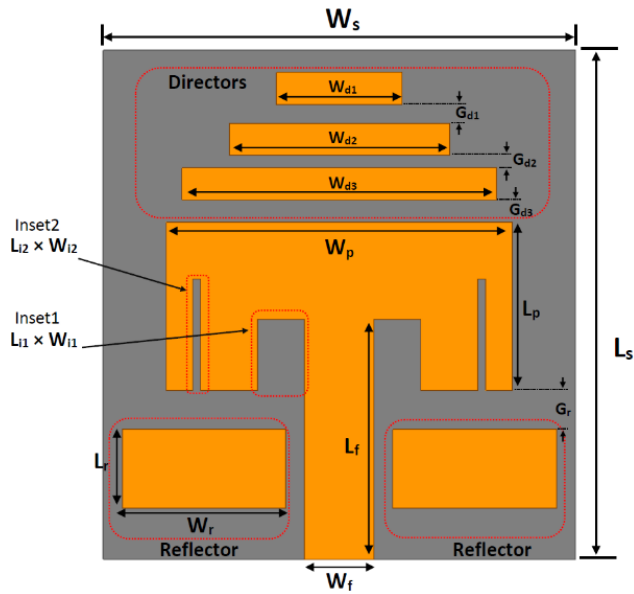
3.1.1 Single patch element design

First, the tentative length and width of the patch were calculated as 1.64 and 3.23 mm, respectively, for an operating frequency of 28GHz using equations 2.1 to 2.5. However, to achieve the desired result of high bandwidth, the parameters of the single patch element were drastically optimized to 5.3 mm \times 11 mm ($L_p \times W_p$). The thickness of the microstrip patch was 1.6 mm, and the overall parameter of the proposed single patch element was 16 mm \times 15 mm \times 1.6 mm. The microstrip patch was designed on a substrate of Taconic RF-45 that has a dielectric constant (ϵ_r) 4.5 and loss tangent 0.0037.

In the initial design, a single rectangular patch element with a simple feedline was designed with an inset of size 2.25 mm \times 1.5 mm, and a continuous ground plane. Then, additional insets of size 3.5 mm \times 0.25 mm were made on each side of the rectangular patch as seen in Fig. 3-1(a). The addition of insets on the patch helped in achieving the operating frequency band of 28GHz. Yagi elements were also added to the design to improve the bandwidth and overall gain. A pair of reflector elements were placed below the patch, and three director elements were placed above the patch. The distance between director and reflector elements were adjusted to achieve the desirable results. The geometry of the finalized single patch element with Yagi elements is shown in Fig. 3-1(b), and its dimensions are listed in Table 1.



(a)



(b)

Figure 3-1. Geometry of single patch element (a) without Yagi elements, (b) with Yagi elements

Table 1. Dimensions of the single patch element

	Parameters	mm
Substrate	$L_s \times W_s$	16×15
Patch	$L_p \times W_p$	5.3×11
Ground	$L_g \times W_g$	16×15
Feedline	$L_f \times W_f$	7.55×2.2
Insets	$L_{i1} \times W_{i1}$	2.25×1.5
	$L_{i2} \times W_{i2}$	3.5×0.25
Reflector element	$L_r \times W_r$	2.5×5.2
	G_r	1.2
Director elements	W_{d1}, W_{d2}, W_{d3}	4, 7, 10
	L_d	1
	G_{d1}, G_{d2}, G_{d3}	0.6, 0.4, 0.7

3.1.2 Comparison of single patch element results

The proposed single patch element was designed and simulated using the Ansoft High-Frequency Structure Simulator (HFSS), which is a commercial electromagnetic simulator. As observed from the results obtained after the simulation in Fig. 3-2, the operating frequency of the microstrip patch is around 28GHz. Fig. 3-2 presents the S_{11} of single-element with and without Yagi elements. As seen in the figure, the return loss of the single patch element antenna is improved by the addition of Yagi elements. Fig. 3-3 shows the VSWR of the single patch element, and as seen from the figure, the single patch is operational from 26.7GHz to 28.78GHz without Yagi elements and from 25.5GHz to 30.64GHz with Yagi elements. The bandwidth of the single

patch element is wider in comparison with the bandwidth achieved by the patch without Yagi elements.

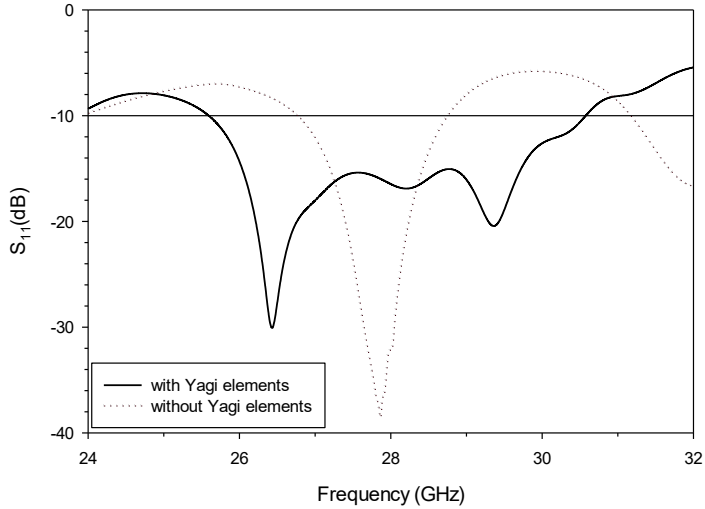


Figure 3-2. S_{11} plot of single patch element with and without Yagi elements

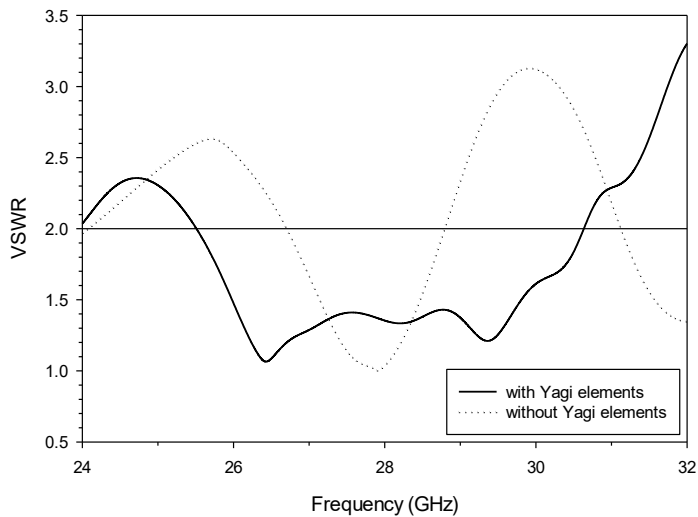


Figure 3-3. VSWR of single patch element with and without Yagi elements

Figure 3-4 shows the radiation pattern of the single patch with Yagi elements at 26.4GHz, 28GHz, and 29.4GHz. As seen from the plots, the proposed single patch element antenna with Yagi elements exhibit a slightly omnidirectional nature.

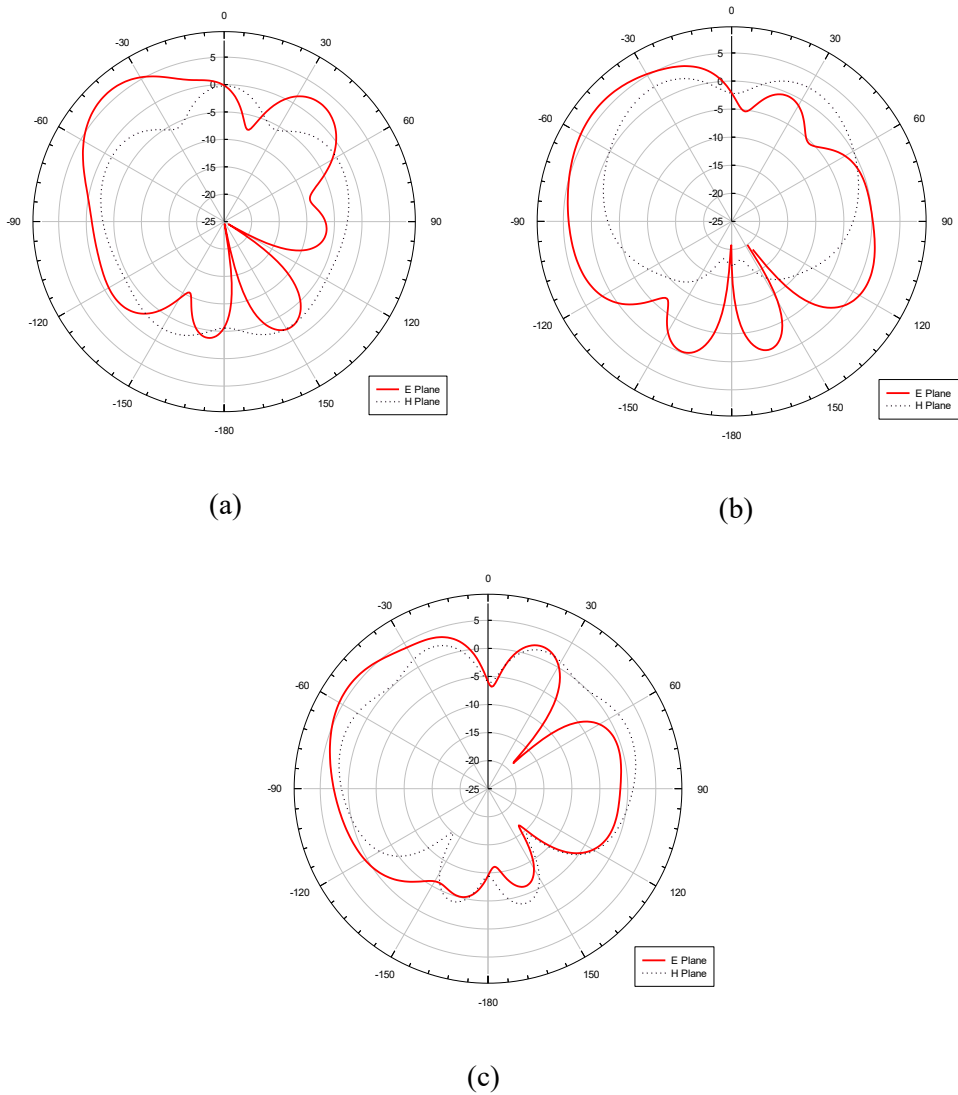


Figure 3-4. Radiation patter of single patch element with Yagi elements (a) at 26.4GHz, (b) at 28GHz, and (c) at 29.4GHz

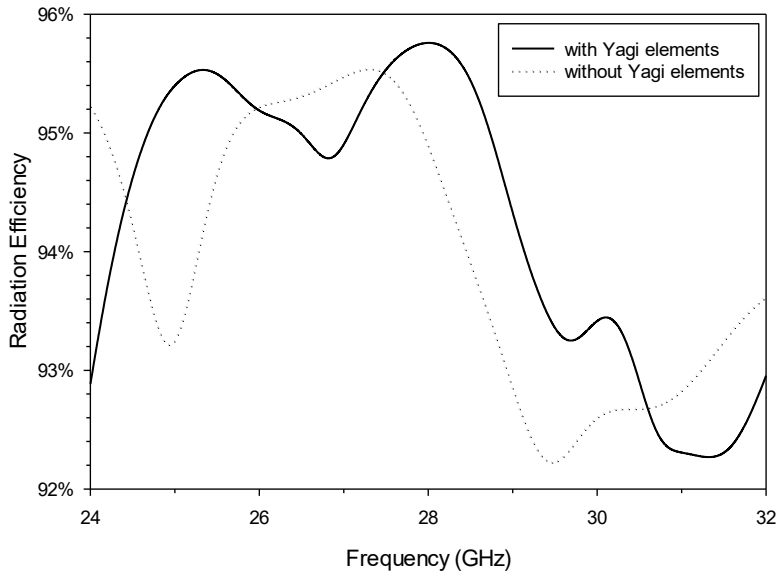


Figure 3-5. Radiation efficiency of single patch element with and without Yagi elements

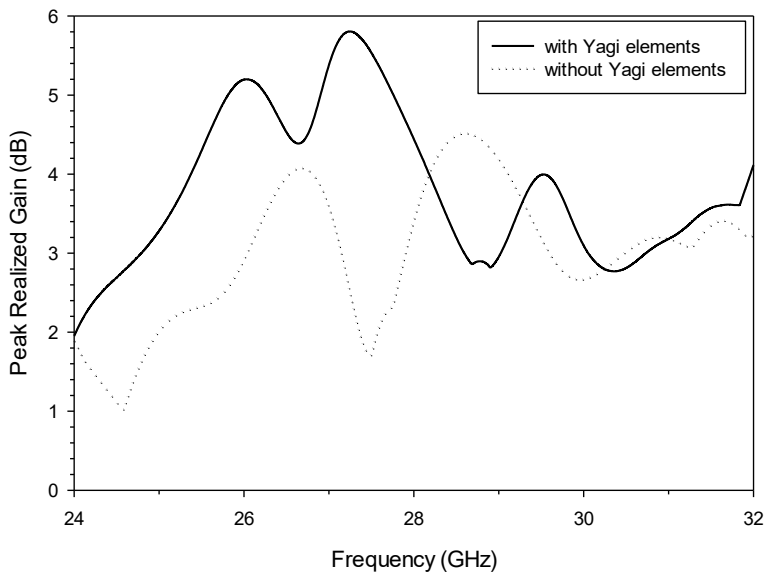


Figure 3-6. Peak realized gain of single patch element with and without Yagi elements

Figure 3-5 presents the radiation efficiency of the single patch element with and without Yagi elements. As seen from the figure, both single patches with and without Yagi elements, have good radiation efficiency around the operating bandwidth. The addition of Yagi elements have also improved the realized gain of the patch element in the targeted operating frequency band with a peak-realized gain of 5.8 dB at 27.4GHz, as seen in Fig. 3-6.

3.2 Array antenna with series feed network

3.2.1 Series-fed array antenna design

After designing a single patch element that achieved the targeted antenna performance, patch elements were combined in the next step to form an array. In our first experiment, we combined four patch elements to form an array using a series feed network. The first patch is fed with a microstrip feedline of width 2.2 mm (W_f), which is the same as that of single element. The remaining three patches were subsequently fed through an optimized thin stub of width 0.2 mm (one-tenth of the size of the feedline, i.e., $W_f/10$). The parameters of each single patch are unchanged, whereas only the size of the overall antenna is changed.

All the patch elements are arranged in series; they are separated by a distance of stub length (L_{st}). Different parameters for the length of the stub were tested to achieve wide bandwidth. Yagi elements of size similar to the ones of single patch element were also added in the design. Two reflector elements were placed only below the first patch element close to the microstrip feed. Three director elements were placed only above the last patch element in the series. In addition, *inset1* is present only in the first patch element, while it has been removed from other patches. Thus, we obtained an array antenna with four single patches, Yagi elements and a continuous ground plane capable of operating around the millimeter wave spectrum.

When the patches are arranged in series, the width of the antenna is compromised. In our design, adding more patch elements in series to obtain a bigger array does not increase the width of the antenna. However, the length of the antenna increases drastically, and the antenna performance is affected.

The geometry of the array antenna with a series feed network is shown in Fig. 3-7, and the additional dimensions are listed in Table 2.

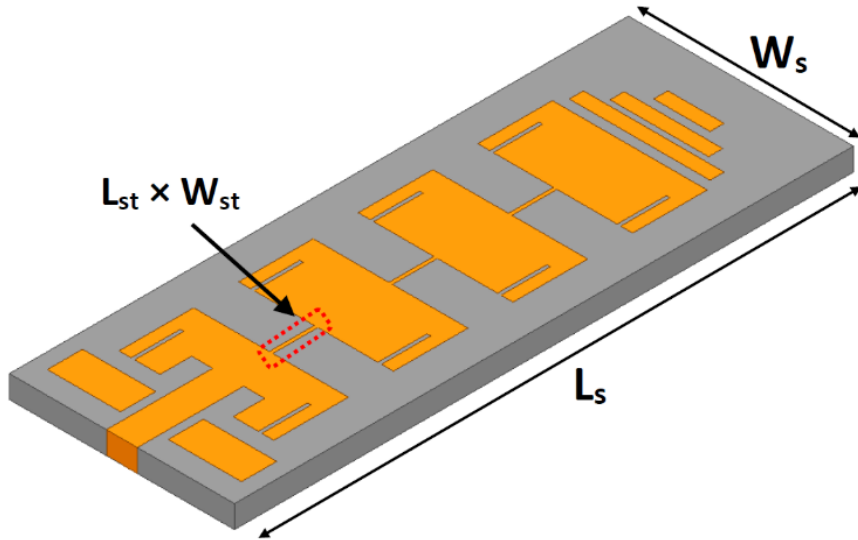


Figure 3-7. Geometry of series-fed microstrip array antenna

Table 2. Dimensions of the series-fed microstrip array antenna

	Parameters	mm
Substrate	$L_s \times W_s$	44×16
Stubs	L_{st}	3.2
	W_{st}	$0.2 (W_f/10)$

3.2.2 Comparison of series-fed array antenna results

Four element array antenna fed with the series feed technique with Yagi elements was designed and simulated in HFSS. The array antenna was simulated with different stub lengths. The stub length in which the bandwidth performance of the antenna was wide was chosen. As seen in Fig. 3-8, S_{11} of

the array antenna with stub lengths 2.2mm, 3.2mm, 4.2mm, and 5.2mm are shown. The return loss for the array antenna with stub length else than 3.2mm produced comparatively narrower bands. Though the return loss is higher for stub lengths 4.2mm and 5.2mm, the bandwidth covered is narrower. Since, the target of the thesis is to achieve wider bandwidth, stub length 3.2mm was chosen for the antenna, which produced bandwidth of 25.6~30.3GHz.

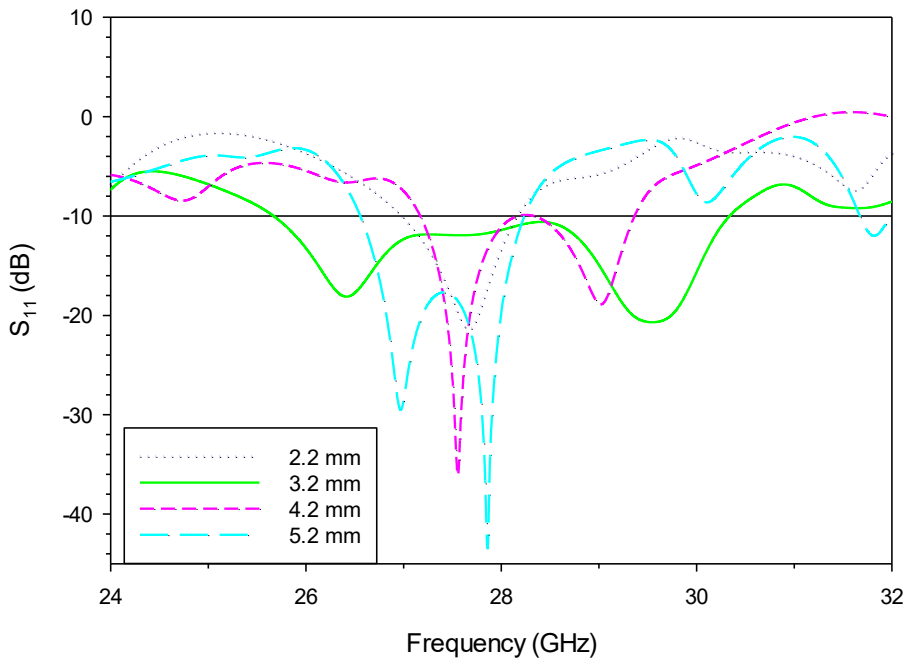


Figure 3-8. S_{11} of series-fed microstrip array antenna with stub lengths 2.2mm, 3.2mm, 4.2mm, and 5.2mm

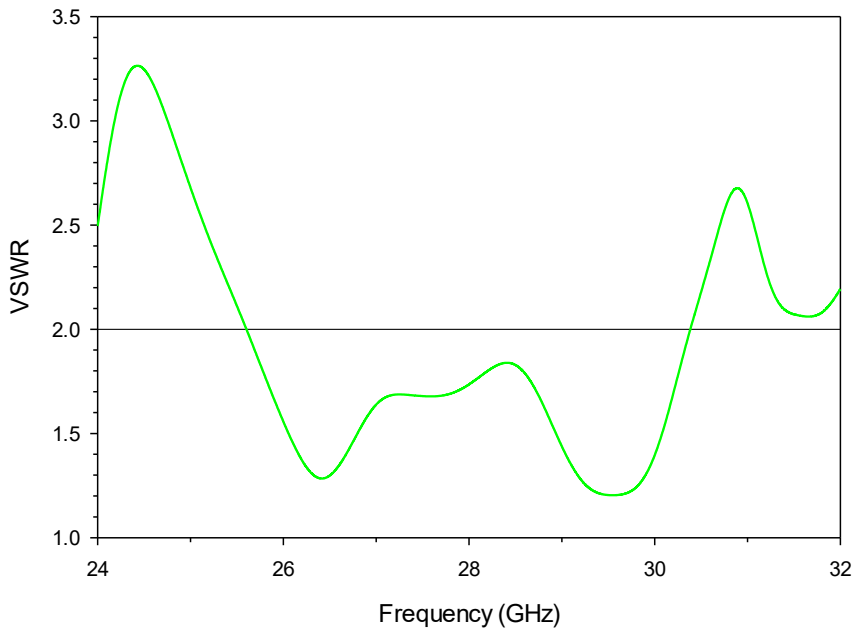


Figure 3-9. VSWR of series-fed microstrip array antenna (with stub length 3.2mm)

Figure 3-9 shows the VSWR of the array antenna with series feed for the chosen stub length of 3.2mm, and as seen from the figure, VSWR is less than 2 for the operating frequency bandwidth of 25.6~30.3GHz. Fig. 3-10 shows the radiation patterns of the array antenna at 26.4GHz, 28GHz, and 29.4GHz. As seen from the plot, the antenna exhibits slight directional nature with Yagi elements added.

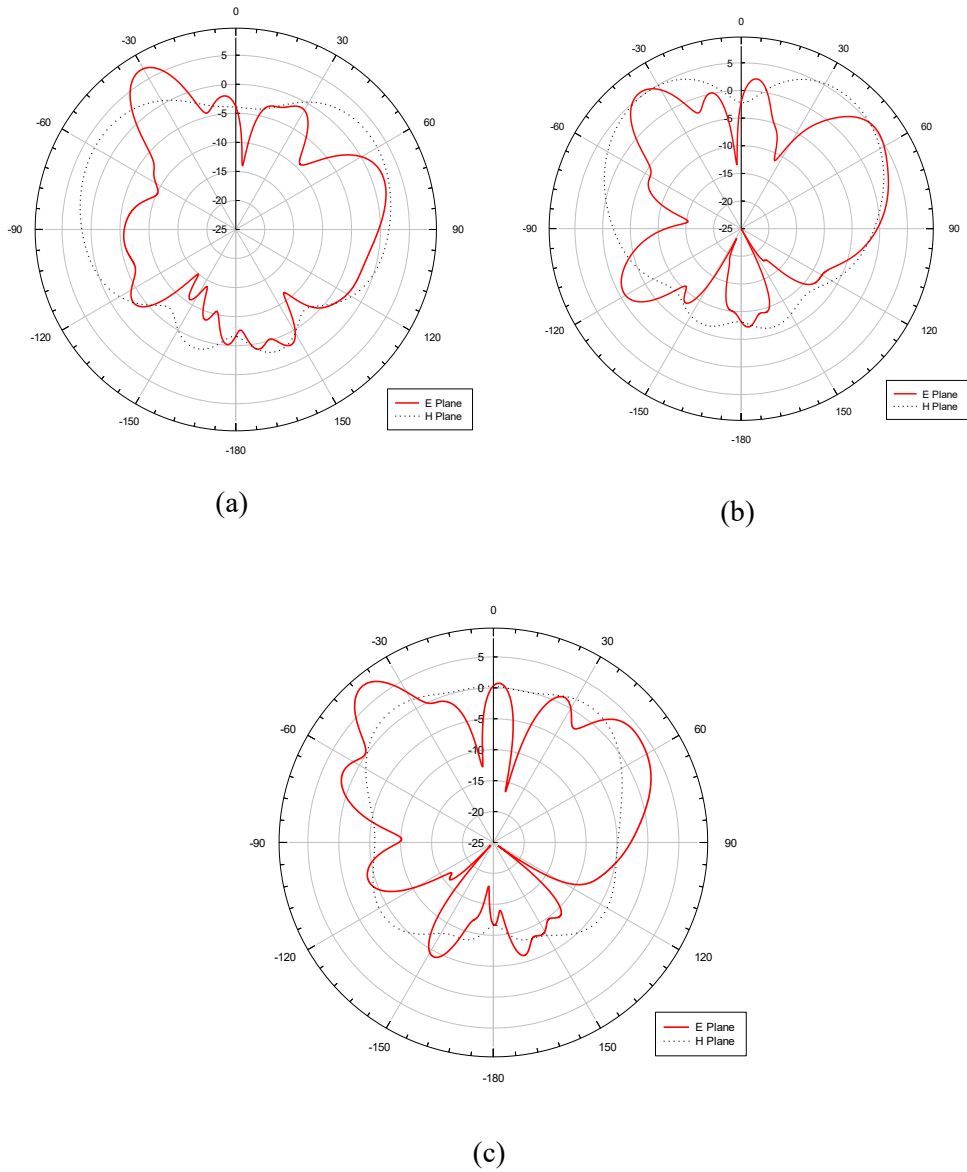


Figure 3-10. Radiation pattern of series-fed microstrip array antenna (a) at 26.4GHz, (b) at 28GHz, and (c) at 29.4GHz

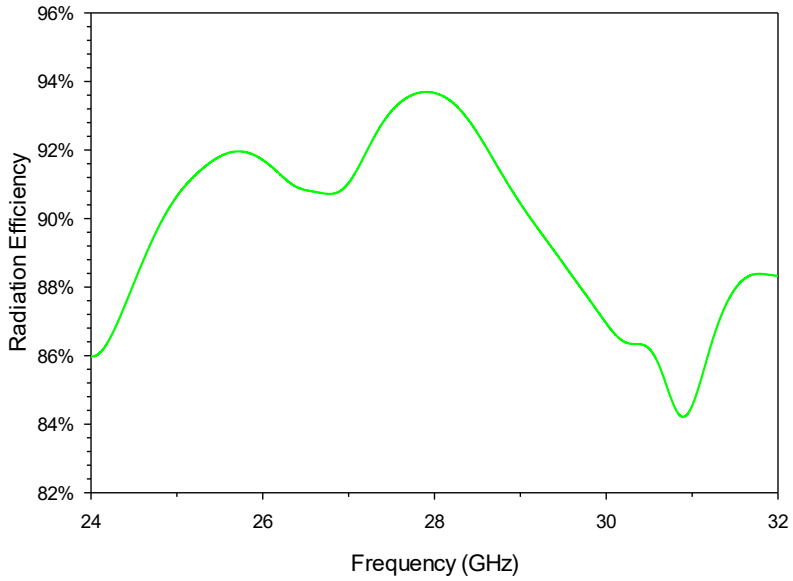


Figure 3-11. Radiation efficiency of series-fed microstrip array antenna

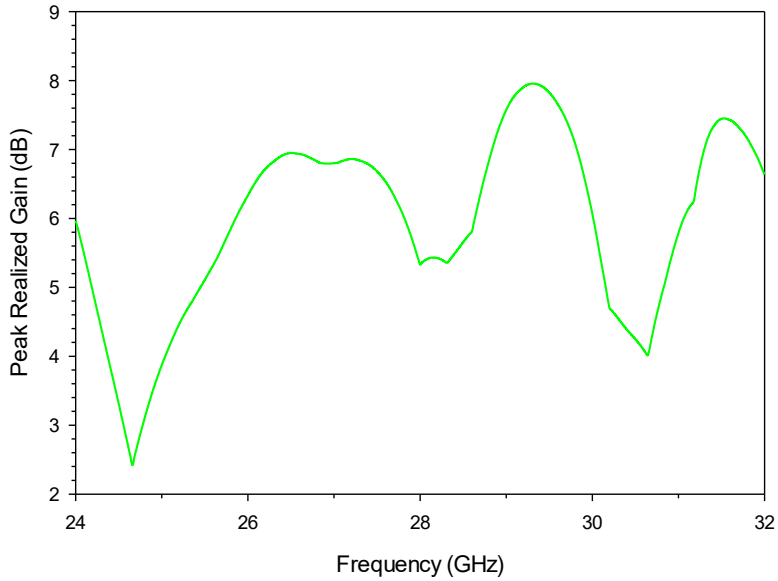


Figure 3-12. Peak realized gain of series-fed microstrip array antenna

Figure 3-11 presents the radiation efficiency of the microstrip array antenna with series feed. As seen from the figure, the antenna has higher radiation efficiency around the operating bandwidth. Fig. 3-12 shows the peak realized gain of the array antenna. The addition of Yagi elements not only increased the bandwidth but also improved the overall gain, with antenna achieving the highest peak realized gain of 8 dB at 29.3GHz. Typically, single patch elements are combined to obtain the final array antenna. Thus, in such cases, the return loss characteristics of an array antenna are similar to those of the single patch elements. In the presented case, although most of the parameters of a single patch element are kept unchanged while designing the array antenna, the placement of Yagi elements in the array antenna is different. While the director elements in a single patch element is above the single patch, director elements are placed only above patch element on the top of array antenna. Similarly, the reflector elements are placed only below first patch of the series array. Because of these changes, the return loss characteristics of the array antenna is different from that of a single patch element.

3.3 Array antenna with corporate feed network

3.3.1 Corporate-fed array antenna design

For the second experiment, four single patch elements are combined to obtain a corporate-fed array antenna. Similar to the series-fed array antenna, the parameters of the single patches and Yagi elements of the corporate-fed array antennas are same.

At first, the feedline was designed for which, by using microstrip formulas, the tentative width of the feedline was estimated around 3.03 mm [38] using the following equations:

$$\frac{w}{h} = \left[\frac{e^H}{8} - \frac{1}{4e^H} \right]^{-1}, \quad (3.1)$$

where

$$H = \frac{Z_0 \sqrt{2(\epsilon_r + 1)}}{119.9} + \frac{1}{2} \left(\frac{\epsilon_r - 1}{\epsilon_r + 1} \right) \left(\ln \frac{\pi}{2} + \frac{1}{\epsilon_r} \ln \frac{4}{\pi} \right). \quad (3.2)$$

Using [39], a tentative length of the microstrip was found as 5.18 mm. In the beginning, the power divider was designed and tested, using the calculated parameters. Later, the parameters were optimized to achieve desirable results. The width of the first feedline was changed from 3.03 mm to 2.2mm, while the width of the second feedline was set to the value of λ_g , i.e. 5 mm. Different lengths of the first feedline were simulated during the design, and the one that resulted in the desirable outputs were selected.

The length of the second feedline is equal to one-fourth of the length of the first feedline (i.e. $L_{f2}=L_{f1}/4$). The T-junction opens into two sections. The total size of the feed of the primary T-junction is 2.2 mm × 30.6 mm, thereby making the distance between two secondary T-junction power dividers almost

equal to $6\lambda_g$. The parameters of the feedlines of the secondary T-junction power divider is the same as that of the primary. Further, two single patch elements are placed on top of each secondary T-junction power divider, thereby making four single patch elements. Here, the distance between the two microstrip patch elements in a secondary T-junction power divider is 17.2mm ($3\lambda_g + \text{feedline width of single patch element}$). The triangular slits are also made in the center of the T-junction to improve the return loss characteristics of the antenna.

The parameters of the single patch element are the same for all. The dimensions of the director elements and reflector elements of the Yagi elements are also same as that of the single patch element. The director elements are placed above every patch elements, whereas the reflector elements are placed only at the open end of the single patch. Thus, each single patch is accompanied by only one reflector element below it. The geometry of the corporate-fed array antenna is shown in Fig. 3-13, and the dimensions are listed in Table 3.

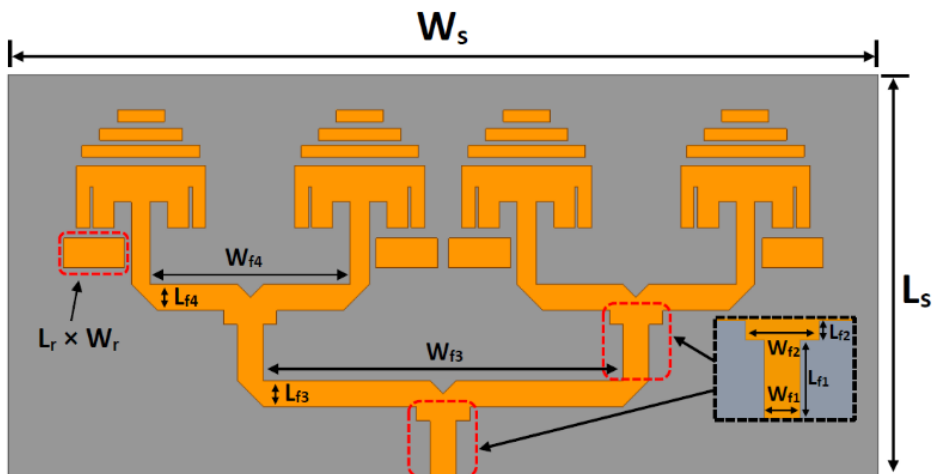


Figure 3-13. Geometry of corporate-fed microstrip array antenna

Table 3. Dimensions of the corporate-fed microstrip array antenna

	Parameters	mm
Substrate	$L_s \times W_s$	36×74
Feedlines	$L_{f1} \times W_{f1}$	4.75×2.2
	$L_{f2} \times W_{f2}$	$1.18 \times 5 (L_{f1}/4 \times \lambda_g)$
	$L_{f3} \times W_{f3}$	2.2×30.6
	$L_{f4} \times W_{f4}$	2.2×17.2
Triangular slit (height \times base)	$L_{f4} \times W_{f4}$	1.1×1.6
Reflector element	$L_r \times W_r$	2.5×5.2

3.3.2 Comparison of corporate-fed array antenna results

The corporate-fed four element array antenna with Yagi elements was designed and simulated in HFSS. Fig. 3-14 shows the return loss of the antenna with different lengths of the first feedline, i.e. L_{f1} . Three different lengths are chosen for the test. At first, antenna is simulated with the feedline length same as the length of the single patch element, i.e. 5.3mm. Then, the antenna is tested with the length of first feedline (L_{f1}) and one-fourth the width of first feedline more or less, i.e. 5.85mm ($L_{f1} + W_{f1}/4$), 4.75mm ($L_{f1} - W_{f1}/4$). The length of the second feedline (L_{f2}) is set one-fourth of the length of the first feedline (i.e. $L_{f2}=L_{f1}/4$). As observed in figure, the return loss of the array antenna produce multiple bandwidths when the lengths of the first feedline are 5.3 mm and 5.85 mm. Thus, the length for the first feedline, L_{f1} , is set as 4.75 mm, in which, the return loss is less than -10 dB from 24.85GHz to 30.32GHz. Fig. 3-15 shows the VSWR of the array antenna with the length of feedline set as 4.75mm, with VSWR less than 2 from 24.85GHz to 30.32GHz.

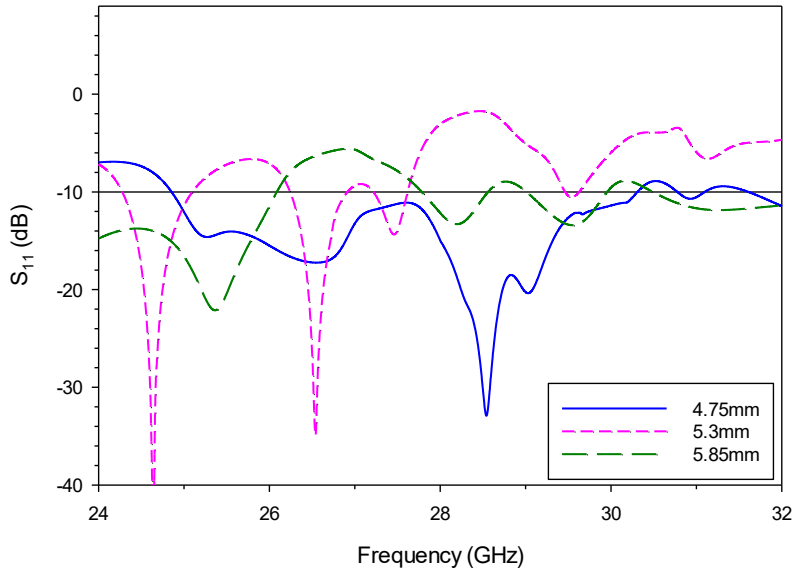


Figure 3-14. S_{11} of corporate-fed microstrip array antenna with feed lengths 4.75mm, 5.3mm, and 5.85mm.

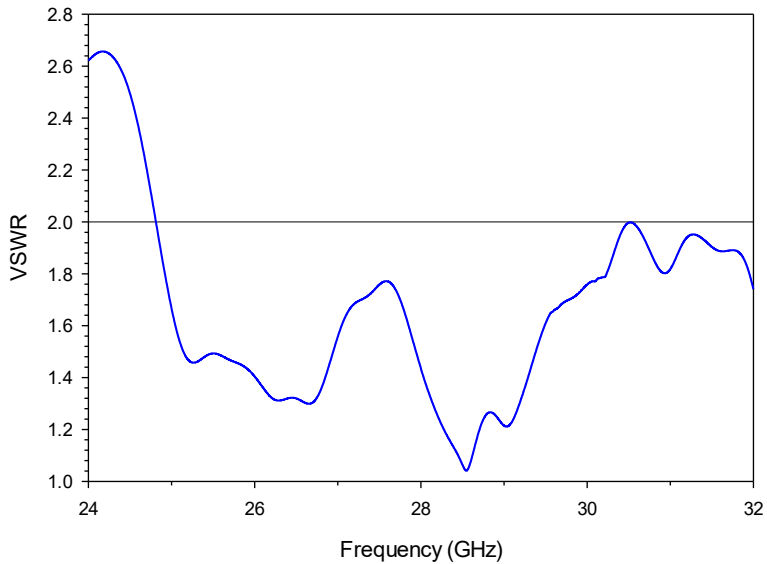


Figure 3-15. VSWR of corporate-fed microstrip array antenna (with feed length 4.75mm)

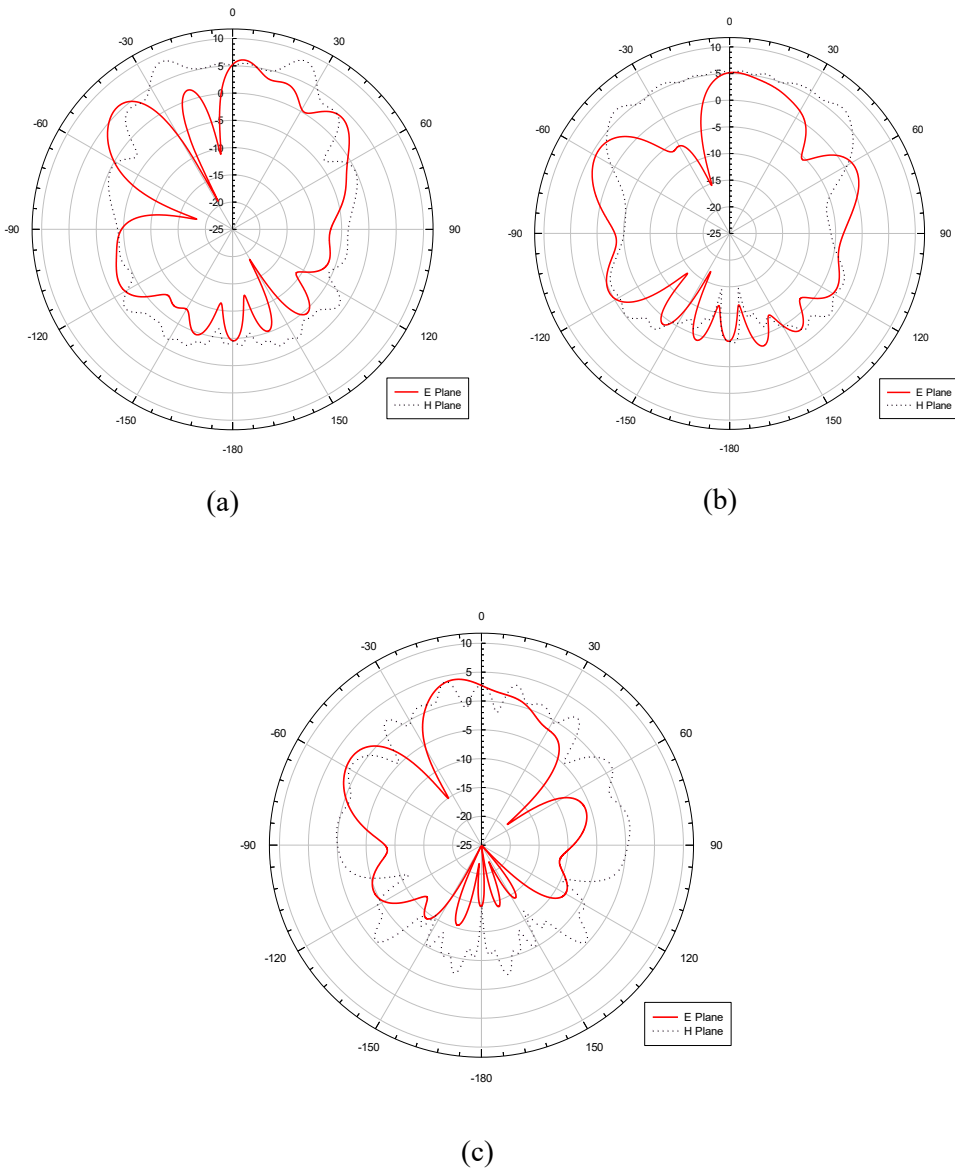


Figure 3-16. Radiation pattern of corporate-fed microstrip array antenna (a) at 26.7GHz, (b) at 28GHz, and (c) at 29.7GHz.

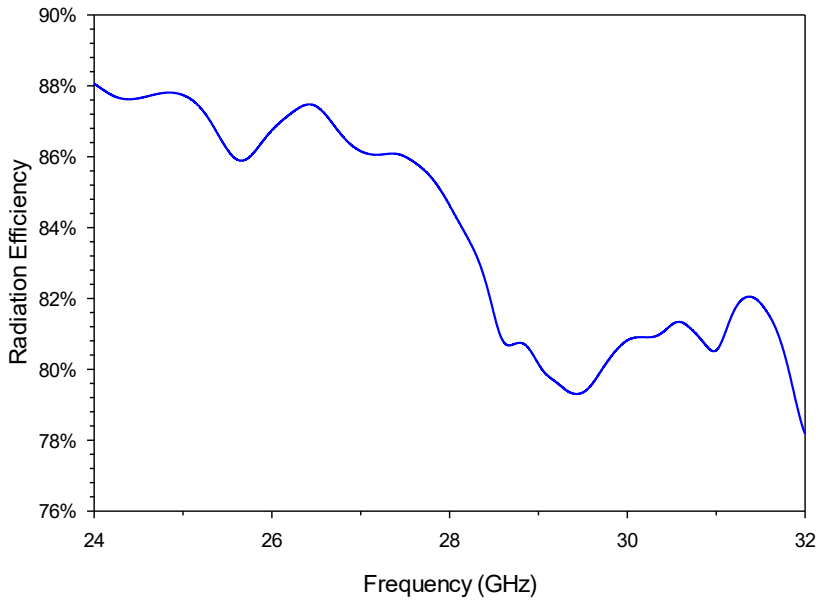


Figure 3-17. Radiation efficiency of corporate-fed microstrip array antenna

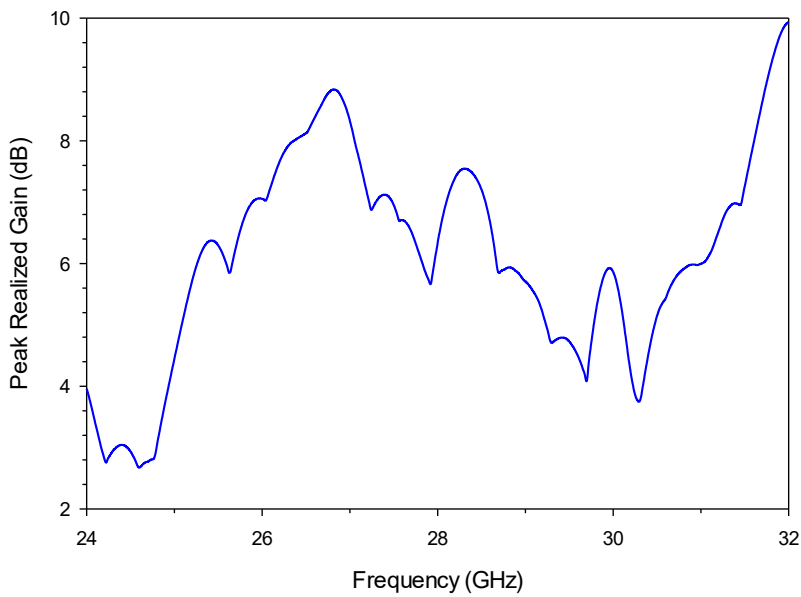


Figure 3-18. Peak realized gain of corporate-fed microstrip array antenna

Figure 3-16 shows the radiation pattern of array antenna with corporate feed network and Yagi elements. As seen from the plots, the antenna exhibits slight directional nature. Fig. 3-17 presents the radiation efficiency of the antenna, and as seen from the figure, the antenna has normal efficiency around the operating bandwidth. However, when compared with the series-fed array antenna, corporate-fed array antenna performs slight lesser. The efficiency of the series-fed array antenna is better than corporate-fed array antenna around the operating bandwidth. Fig. 3-18 shows the peak realized gain, and as seen in the figure, the antenna achieved a highest peak realized gain of 8.8 dB at 26.7GHz (inside the operating bandwidth). The addition of Yagi elements improved the gain of the overall operating region of the antenna.

3.4 Proposed array antenna with corporate-series feed network

3.4.1 Corporate-series-fed array antenna design

After designing and testing series-fed and corporate-fed array antennas with Yagi elements, we finally present a rectangular patch array antenna by combining the corporate and series feeding techniques. Two patch elements are fed equal power of 50-ohm source using a network of a microstrip line in form of the T-junction power divider. Further, patch elements are placed on top of each patch element in series using a quarter wavelength transformer stub.

The parameters of the patch elements are kept unchanged. The dimension of the Yagi elements are also kept same as that in the single patch antenna, series-fed and corporate-fed array antennas. The width and length of the stub is the same as that in the series-fed array antenna. The dimensions of the T-junction power divider is also same as that of the T-junction of corporate-fed array antenna. The combination of series and corporate feeding technique is done to enhance the overall performance of the antenna, decrease the size, increase the bandwidth, and improve the gain of the antenna, thereby making the array antenna suitable for 5G applications. In this way, two feeding techniques (i.e., series and corporate) are combined to obtain a corporate-series feeding technique. This combination of feeding techniques allowed us to design an array antenna of four patch elements without compromising the overall size. The total size of the array antenna is also smaller than that of series- or corporate-fed array antennas. The geometry of the proposed array antenna is shown in Fig. 3-19, and the dimensions are listed in Table 4.

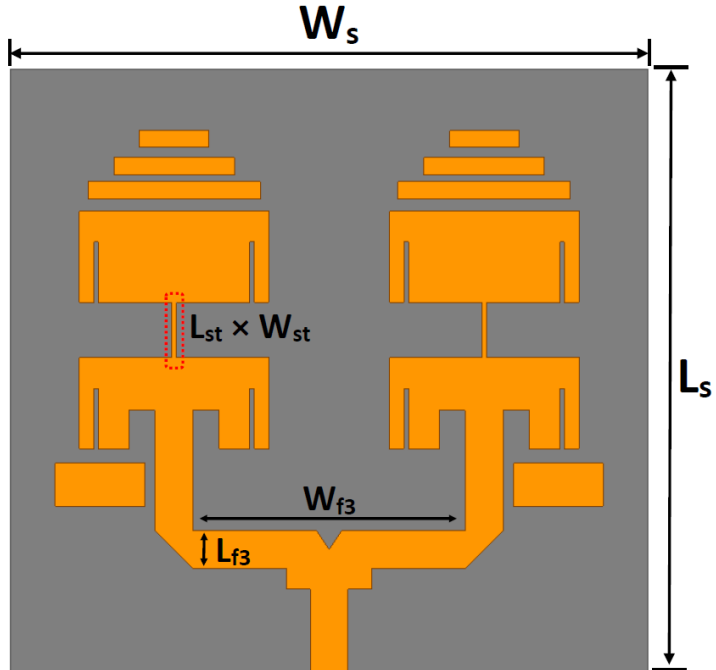


Figure 3-19. Geometry of proposed corporate-series-fed microstrip array antenna

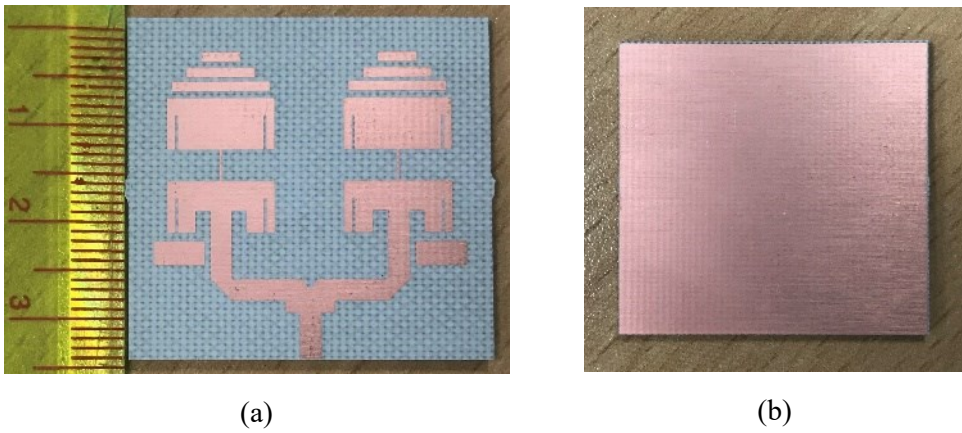


Figure 3-20. Fabricated prototype of proposed corporate-series-fed microstrip array antenna (a) top view, (b) bottom view

Table 4. Dimensions of the proposed microstrip array antenna

	Parameters	mm
Substrate	$L_s \times W_s$	35×37
Feedlines	$L_{f3} \times W_{f3}$	2.2×15.8
Stubs	L_{st}	3.2
	W_{st}	$0.2 (W_f/10)$

3.4.2 Comparison of simulated and measured results

After simulating series- and corporate-fed array antennas, the proposed corporate-series-fed array antenna was finally designed and simulated; next, it was evaluated in a real environment. The measured and simulated S_{11} of the prototypes are presented in Fig. 3-21 along with the simulated results of series- and corporate-fed array antennas. The measured return loss is below -10 dB from 24.89GHz to 30.79GHz. The array operates in a potential band proposed for 5G communication and even exhibits a return loss of approximately -26 dB at 27.8GHz. However, in the simulated result, the return loss is around -48 dB at 27.8GHz and is below -10 dB from 25.4GHz to 30.87GHz. This difference between the measured and simulated result could be due to minor manufacture defect, loss due to the nature of substrate, or loss due to connector. However, as can be observed in the figure, the return loss exhibits a matched behavior along the measured band. Fig. 3-22 presents the simulated VSWR of the proposed microstrip array antenna with corporate-series feed network, and as seen from the figure, the VSWR is less than 2 in the operating frequency bandwidth.

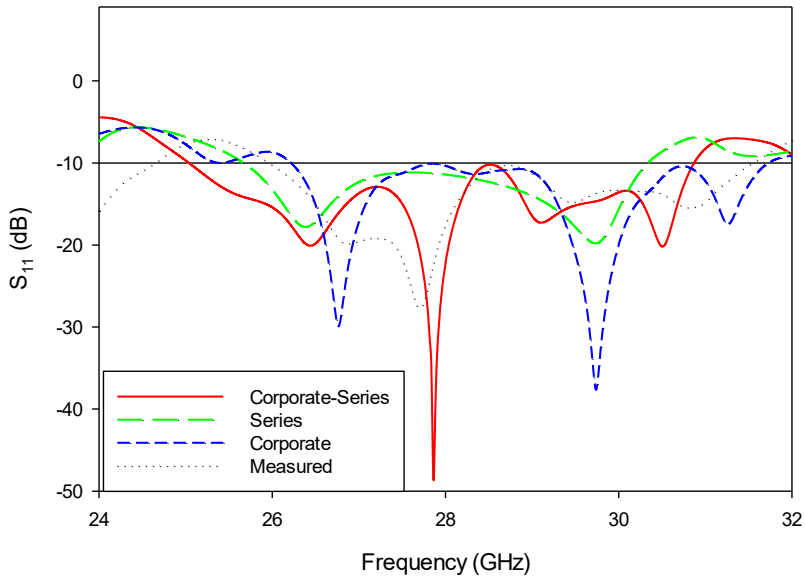


Figure 3-21. Measured and simulated S_{11} of proposed corporate-series-fed microstrip array antenna vs S_{11} of series- and corporate-fed array antennas

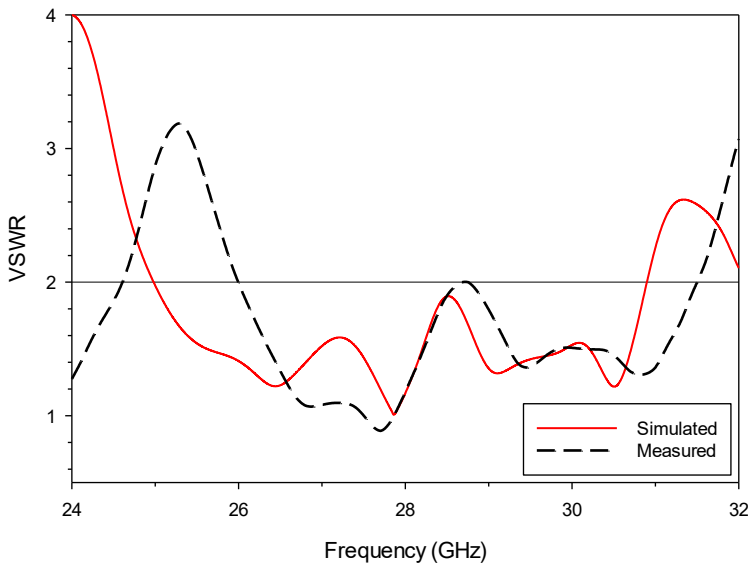


Figure 3-22. Measured and simulated VSWR of proposed corporate-series-fed microstrip array antenna

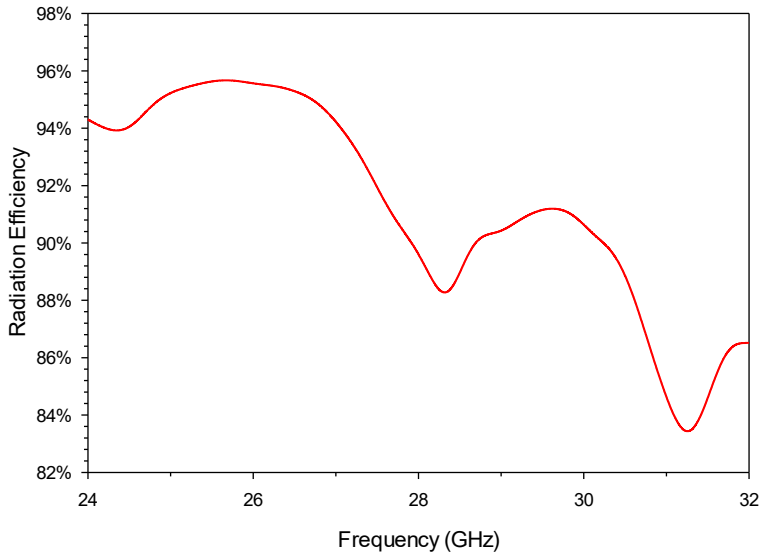


Figure 3-23. Radiation efficiency of proposed corporate-series-fed microstrip array antenna

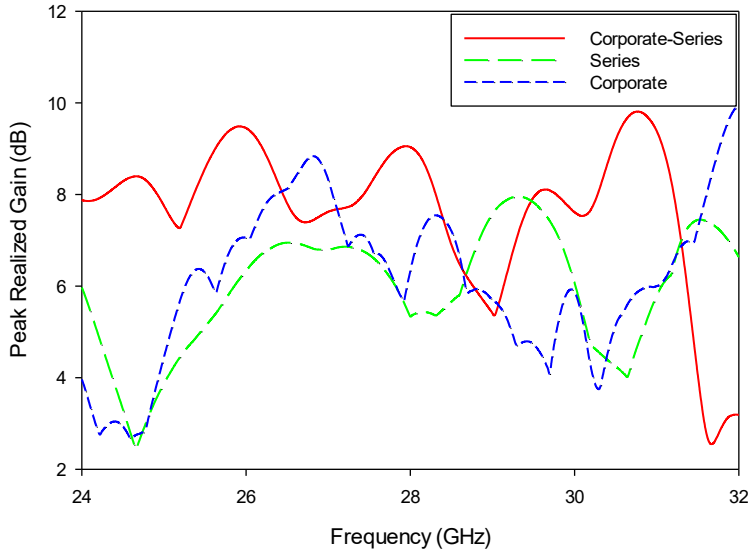


Figure 3-24. Peak realized gain of proposed corporate-series-fed microstrip array antenna vs peak realized gain of series- and corporate-fed array antennas

In Fig. 3-23, radiation efficiency of the antenna is presented. The antenna performs well as the radiation efficiency is greater than 80% throughout the operating frequency bandwidth. Fig. 3-24 depicts simulated results of peak realized gain of the proposed array antenna along with results of series- and corporate-fed array antennas. It can be observed that the realized gain of the proposed antenna over the operating frequency band of the antenna is higher than that of series- or corporate-fed array antennas.

Fig. 3-25 shows the measured and simulated radiation patterns of the proposed corporate-series-fed array antenna at 27GHz, 28GHz, and 29GHz. The measured radiation pattern is represented by broken lines while the simulated result is represented by a smooth straight line. As seen from the plots, the presented antenna exhibit a slight directional nature. However, the measured results show slight shift on the pattern when compared to the simulated radiation patterns. Dissimilarities between the measured and simulated results are due to the loss because of manufacture defect, nature of substrate or measurement errors. In the proposed antenna, the fed power is first equally split at each junction of the patch array with uniform distribution; it passes along the continuous transmission lines through which a proportion of energy is progressively coupled into each element arranged in series. Owing to these reasons, an array antenna with high gain is achieved.

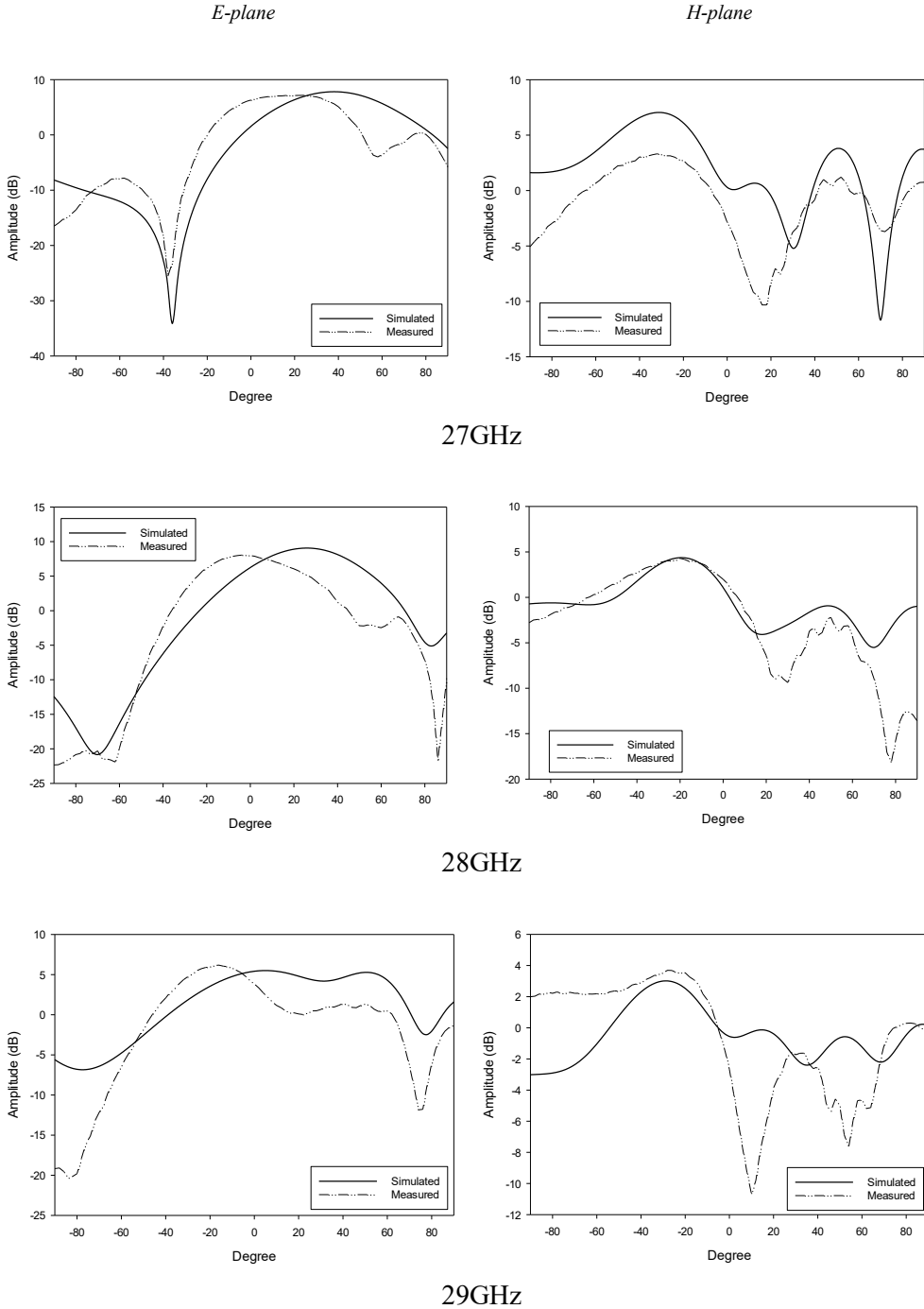


Figure 3-25. Radiation pattern of the proposed corporate-series-fed array antenna at 27GHz, 28GHz, and 29GHz

Table 5 presents the comparison of array antennas with Yagi elements fed by series only, corporate only, and corporate-series feeding techniques in terms of maximum return loss, bandwidth, maximum peak realized gain, and size. The proposed design is also compared with other antenna models. From the comparison table, it is clear that the corporate-series-fed array antenna outperforms the designed series- and corporate-fed array antennas in terms of gain and bandwidth. In addition, the size of the antenna is smaller when the array is fed using the corporate-series feeding technique.

Table 5. Comparison between array antenna models

Antenna type	Max. return loss (dB)	Bandwidth (GHz)	Max. gain (dB)	Size (L_s × W_s) mm²
Series feed	-20.7	25.67~30.34	7.98	44 × 16
Corporate feed	-32.9	24.85~30.32	8.85	36 × 74
Corporate-series feed	-48.6	25.05~30.87	9.49	35 × 37
[19] (Series feed)	≈ -30	27.3~29	14.9	24.3 × 24.3
[18] (Series feed)	≈ -40	27.45~28.95	12.9	78.5 × 42
[20] (Corporate feed)	≈ -50	27.8~28.1	17	39.3 × 30.7
[21] (Corporate-series)	≈ -60	26.4~28.9	17.1	88 × 25

From the table, it is also clear that the proposed antenna has much wider bandwidth than other microstrip antenna models fed with either series,

corporate or combined corporate-series feeding techniques, proposed by various researchers for 5G application, which meets the target of the thesis. The proposed array antenna is smaller than all the compared models except [19]. Though the presented corporate-series fed array antenna performs well in terms of bandwidth and size than the array antenna models in comparison, the gain obtained by other models is higher. However, the gain achieved by the array antenna is acceptable and is a room for improvement in the future work.

3.5 Corporate-series-fed array antenna on FR4 substrate

3.5.1 Design of array antenna on FR4 substrate

The array antenna proposed in this thesis was designed on Taconic substrate. However, during the research, corporate-series-fed microstrip array antenna was also designed on FR4 substrate in similar manner as the proposed array antenna. The dielectric constant (ϵ_r) of the FR4 substrate is 4.4 and loss tangent is 0.02. The dielectric constant of Taconic RF-45 substrate used to build the proposed array antenna is 4.5 and loss tangent is 0.0037. Both substrates are easily available.

The design procedure followed similar process: at first, the single patch was designed. The single patch element design was same with variation in parameters. The geometry of the single patch element with Yagi elements built on FR4 substrate is shown in Fig. 3-26, and the dimensions of the patch are listed in Table 6.

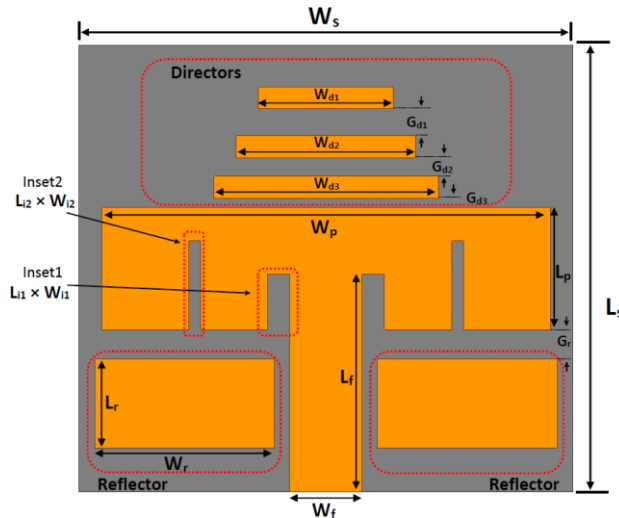


Figure 3-26. Geometry of single patch element on FR4 substrate

Table 6. Dimensions of the single patch in FR4 substrate

	Parameters	mm
Substrate	$L_s \times W_s$	10×11
Patch	$L_p \times W_p$	2.75×8
Ground	$L_g \times W_g$	10×11
Feedline	$L_f \times W_f$	4.875×1.6
Insets	$L_{i1} \times W_{i1}$	1.25×0.5
	$L_{i2} \times W_{i2}$	2×0.25
Reflector element	$L_r \times W_r$	2×4
	G_r	0.475
Director elements	W_{d1}, W_{d2}, W_{d3}	3, 4, 5
	L_d	0.5
	G_{d1}, G_{d2}, G_{d3}	0.6, 0.4, 0.2

The process followed with the design of series- and corporate-fed array antennas, finally, concluding at the corporate-series-fed array antenna. The geometry of the final corporate-series-fed array antenna designed on FR4 is shown in Fig. 3-27, followed by the fabricated prototype in Fig. 3-28, with the remaining dimensions listed in Table 7.

The design of the final array antenna built on the FR4 substrate is smaller in dimension compared to array antenna on Taconic substrate. While the total size of array antenna on FR4 is $22 \text{ mm} \times 28 \text{ mm}$, the total size on Taconic is $35 \text{ mm} \times 37 \text{ mm}$. The array antenna built on Taconic (1295 mm^2) is double the size of array antenna on FR4 (616 mm^2). Thus, FR4 has advantage over Taconic in terms of size.

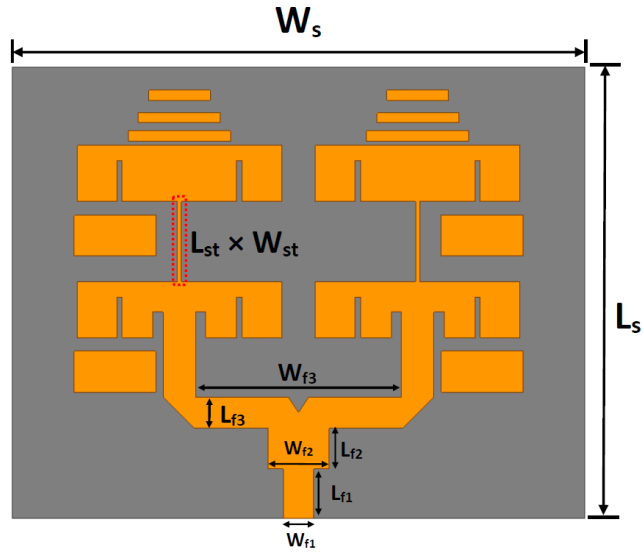
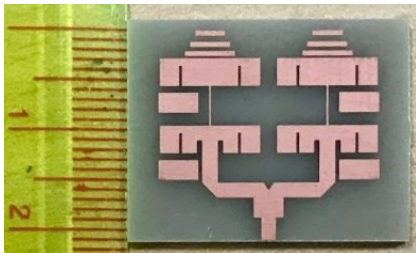
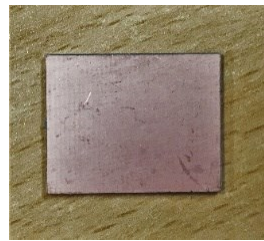


Figure 3-27. Geometry of corporate-series-fed microstrip array antenna on FR4 substrate



(a)



(b)

Figure 3-28. Fabricated prototype of corporate-series-fed microstrip array antenna on FR4 substrate (a) top view, (b) bottom view

Table 7. Dimensions of the array antenna on FR4 substrate

	Parameters	mm
Substrate	$L_s \times W_s$	22×28
Feedlines	$L_{f1} \times W_{f1}$	2.4×1.5
	$L_{f2} \times W_{f2}$	2×3
	$L_{f3} \times W_B$	1.5×10.25
Stubs	L_{st}	$3.9\{(\lambda_g/2) + L_{i1}\}$
	W_{st}	$0.2 (W_f/8)$

3.5.2 Comparison of results between FR4 and Taconic

The final array antenna designed on FR4 substrate was also simulated in HFSS and later fabricated, and the parameters were measured in real environment. The measured and simulated S_{11} of the FR4 prototypes are presented in Fig. 3-29 along with the measured and simulated results of proposed Taconic array antenna. As seen from the figure, the simulated return loss of both the antennas are similar, operating at frequency band around 28GHz. While the bandwidth of Taconic antenna based on simulated result is from 25.05GHz to 30.87GHz, the bandwidth of FR4 antenna is even wider, from 23.97GHz to 31.60GHz. However, there are differences in the measured results. In case of Taconic antenna, the measured result is similar to the simulated result. In case of FR4, the measured result is nowhere close to the simulated result. The measured result of FR4 array antenna suggests that antenna cannot operate in the frequency band of 28GHz. The huge difference in the simulated and measured result of FR4 array antenna might have been caused due to the nature of FR4 substrate, as it is susceptible to high loss when

operating in higher frequency bands. Manufacture defects and loss due to connector might also be other reasons for the undesirable measured results.

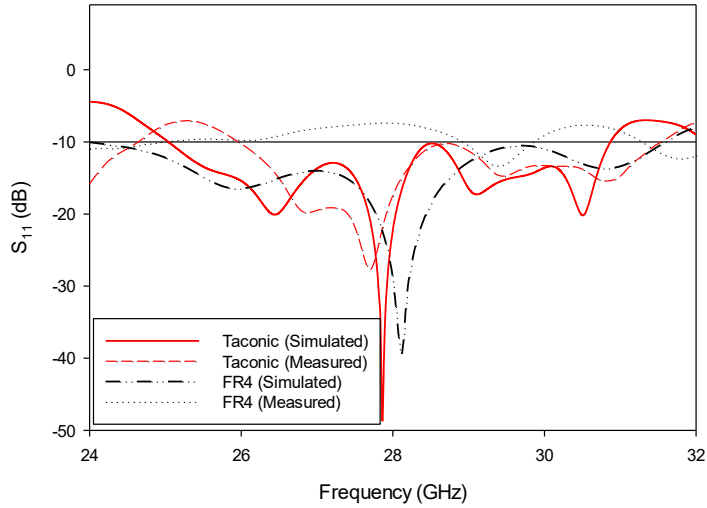


Figure 3-29. Measured and simulated S_{11} of corporate-series-fed microstrip array antennas on Taconic substrate vs on FR4 substrate

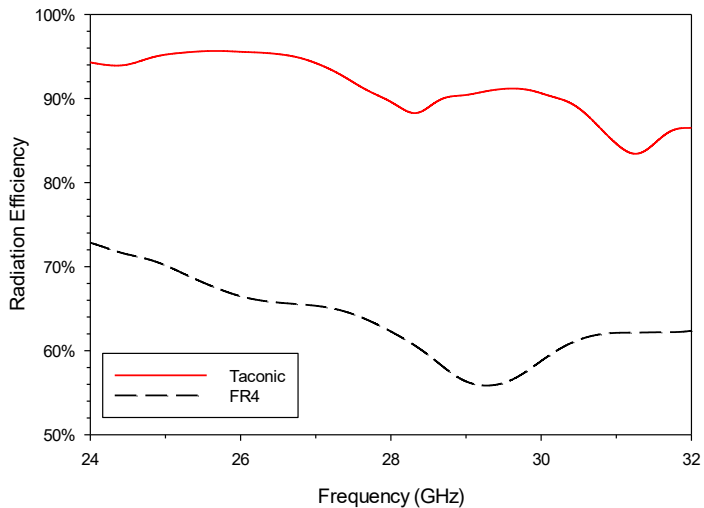


Figure 3-30. Radiation efficiencies of corporate-series-fed microstrip array antennas on Taconic substrate vs on FR4 substrate

In Fig. 3-30, radiation efficiencies of both array antennas are presented. As seen from the figure, array antenna built on Taconic substrate has radiation efficiency higher than 80% throughout the operating bandwidth. Whereas, array antenna on FR4 substrate's radiation efficiency is even below 70% around the operating bandwidth.

Thus, array antenna on Taconic substrate performed better in terms of real environment and radiation efficiency than array antenna on FR4 substrate. Due to these reasons, the proposed design was built using the Taconic substrate. Further, FR4 substrate is not recommended while designing antenna systems for higher frequency bands.

4. Conclusion

In this thesis, an efficient array antenna design of a simple microstrip patch for 5G communication with wide bandwidth covering most of the higher 5G bands is proposed. The proposed array antenna with the corporate-series feed network was the result of combining two different feeding techniques: series and corporate. Prior to designing the proposed array antenna, the thesis presented the design of single patch element operating at 28GHz frequency band, which is part of 5G communication. The single patch element was designed with and without Yagi elements, showing how the addition of the Yagi elements improved overall gain and extended the bandwidth. Then after, four single patch elements were combined to form two array antennas with different feeding techniques.

In the first array antenna, series feeding technique was used. The series-fed microstrip array antenna resulted with maximum gain of 7.98 dB and operating frequency bandwidth of 25.67~30.34GHz. The second array antenna, corporate-fed microstrip array antenna, yielded an output of maximum gain of 8.85 dB and bandwidth of 24.85~30.32GHz. Finally, the two feeding techniques were combined and the proposed array antenna was designed with corporate-series feeding technique. The antenna achieved highest gain of 9.49 dB and operating frequency bandwidth of 25.05~30.87GHz. Further, proposed design was compared with series- and corporate-fed array antennas. Overall, the simulation results proved that the proposed microstrip array antenna outperformed the series- and corporate-fed array antennas in terms of antenna gain, and size. In addition, the design was built on Taconic substrate. The substrate was chosen instead of FR4, after comparing the measured and simulated results of antenna designs built on both Taconic and FR4.

Overall, the proposed microstrip patch array antenna with corporate-series feed and Yagi elements on Taconic substrate is suitable for IoTs and 5G communication systems.

Acknowledgement

I would like to express my deepest gratitude to my advisor, Prof. Dong-You Choi, at Chosun University, for his support and inspiration throughout my graduate studies. He was always kind and patient with me whenever I ran into troubles or had questions related to my research. His technical and editorial advice and guidelines were important to complete this research.

I would also like to thank my lab seniors Mr. Jiwan Ghimire and Dr. Sun-Woong Kim. The research idea would not have taken shape without their passionate participation, valuable suggestions and generous assistance. The two valuable years spent in the lab has been fruitful because of their presence.

Finally, I would like to express my deep appreciation to my friends for their love, understanding, and encouragement during the period of this research.

References

- [1] T. S. Rappaport, S. Sun, R. Mayzus, H. Zhao, Y. Azar, K. Wang, G. N. Wong, J. K. Schulz, M. Samimi, and F. Gutierrez, “Millimeter wave mobile communications for 5G cellular: It will work!,” *IEEE access*, vol. 1, pp. 335–349, 2013.
- [2] T. S. Rappaport, J. N. Murdock, and F. Gutierrez, “State of the art in 60-GHz integrated circuits and systems for wireless communications,” *Proceedings of the IEEE*, vol. 99, no. 8, pp. 1390–1436, 2011.
- [3] Z. Pi and F. Khan, “An introduction to millimeter-wave mobile broadband systems,” *IEEE communications magazine*, vol. 49, no. 6, pp. 101–107, 2011.
- [4] T. Kim, I. Bang, and D. K. Sung, “Design criteria on a mmWave-based small cell with directional antennas,” 2014 IEEE 25th Annual International Symposium on Personal, Indoor, and Mobile Radio Communication (PIMRC), pp. 103–107, 2014.
- [5] R. A. Alhalabi, “High efficiency planar and RFIC-based antennas for millimeter-wave communication systems,” 2010.
- [6] E. U. T. R. Access, “User Equipment (UE) radio transmission and reception,” *3GPP TS*, vol. 36, pp. V10, 2010.
- [7] S. F. Jilani, Q. H. Abbasi, and A. Alomainy, “Inkjet-Printed Millimetre-Wave PET-Based Flexible Antenna for 5G Wireless Applications,” 2018 IEEE MTT-S International Microwave Workshop Series on 5G Hardware and System Technologies (IMWS-5G), pp. 1–3, 2018.
- [8] Y. Rahayu and M. I. Hidayat, “Design of 28/38 GHz Dual-Band Triangular-Shaped Slot Microstrip Antenna Array for 5G Applications,” 2018 2nd International Conference on Telematics and Future Generation Networks (TAFGEN), pp. 93–97, 2018.
- [9] H. A. Diawuo and Y.-B. Jung, “Broadband Proximity-Coupled Microstrip Planar Antenna Array for 5G Cellular Applications,” *IEEE Antennas and Wireless Propagation Letters*, vol. 17, no. 7, pp. 1286–1290, 2018.
- [10] H. Aliakbari, A. Abdipour, R. Mirzavand, A. Costanzo, and P. Mousavi, “A single feed dual-band circularly polarized millimeter-wave antenna

- for 5G communication,” 2016 10th European Conference on Antennas and Propagation (EuCAP), pp. 1–5, 2016.
- [11] O. M. Haraz, M. M. M. Ali, S. Alshebeili, and A.-R. Sebak, “Design of a 28/38 GHz dual-band printed slot antenna for the future 5G mobile communication networks,” 2015 IEEE International Symposium on Antennas and Propagation & USNC/URSI National Radio Science Meeting, pp. 1532–1533, 2015.
- [12] J. Qiao, “Enabling Millimeter Wave Communication for 5G Cellular Networks: MAC-layer Perspective,” 2015.
- [13] M. A. Sohaib, S. Bashir, S. ur Rehman, and F. Azam, “High gain microstrip yagi antenna for millimeter waves,” 2018 International Conference on Computing, Mathematics and Engineering Technologies (iCoMET), pp. 1–4, 2018.
- [14] H. Zhao, R. Mayzus, S. Sun, M. Samimi, J. K. Schulz, Y. Azar, K. Wang, G. N. Wong, F. Gutierrez, and T. S. Rappaport, “28 GHz millimeter wave cellular communication measurements for reflection and penetration loss in and around buildings in New York city,” 2013 IEEE International Conference on Communications (ICC), pp. 5163–5167, 2013.
- [15] G. R. MacCartney, J. Zhang, S. Nie, and T. S. Rappaport, “Path loss models for 5G millimeter wave propagation channels in urban microcells,” Globecom, pp. 3948–3953, 2013.
- [16] H. Errifi, A. Baghdad, A. Badri, and A. Sahel, “Design and analysis of directive microstrip patch array antennas with series, corporate and series-corporate feed network,” *International Journal of Electronics and Electrical Engineering*, vol. 3, no. 6, pp. 416–423, 2015.
- [17] F.-Y. Kuo and R.-B. Hwang, “High-isolation X-band marine radar antenna design,” *IEEE Transactions on Antennas and Propagation*, vol. 62, no. 5, pp. 2331–2337, 2014.
- [18] T. Varum, A. Ramos, and J. N. Matos, “Planar microstrip series-fed array for 5G applications with beamforming capabilities,” 2018 IEEE MTT-S International Microwave Workshop Series on 5G Hardware and System Technologies (IMWS-5G), pp. 1–3, 2018.
- [19] M. Khalily, R. Tafazolli, T. A. Rahman, and M. R. Kamarudin, “Design of phased arrays of series-fed patch antennas with reduced number of the

- controllers for 28-GHz mm-wave applications,” *IEEE Antennas and Wireless Propagation Letters*, vol. 15, pp. 1305–1308, 2015.
- [20] D. N. Arizaca-Cusicuna, J. L. Arizaca-Cusicuna, and M. Clemente-Arenas, “High Gain 4x4 Rectangular Patch Antenna Array at 28GHz for Future 5G Applications,” 2018 IEEE XXV International Conference on Electronics, Electrical Engineering and Computing (INTERCON), pp. 1–4, 2018.
- [21] B. T. Mohamed and H. Ammor, “A 16-elements Corporate-series Feed Rectangular Patch Antenna Array at 28GHz, for future 5G applications,” 2019 International Conference on Wireless Technologies, Embedded and Intelligent Systems (WITS), pp. 1–4, 2019.
- [22] R. Waterhouse, “Printed antennas for wireless communications,” *John Wiley & Sons*, 2008.
- [23] F.-J. Huang, C.-M. Lee, C.-Y. Kuo, and C.-H. Luo, “MMW antenna in IPD process for 60-GHz WPAN applications,” *IEEE Antennas and Wireless Propagation Letters*, vol. 10, pp. 565–568, 2011.
- [24] A. Agarwal, G. Misra, and K. Agarwal, “The 5th generation mobile wireless networks-key concepts, network architecture and challenges,” *American Journal of Electrical and Electronic Engineering*, vol. 3, no. 2, pp. 22–28, 2015.
- [25] F. Boccardi, R. W. Heath, A. Lozano, T. L. Marzetta, and P. Popovski, “Five disruptive technology directions for 5G,” *IEEE communications magazine*, vol. 52, no. 2, pp. 74–80, 2014.
- [26] M. Series, “Future technology trends of terrestrial IMT systems,” 2015.
- [27] I. Chih-Lin, C. Rowell, S. Han, Z. Xu, G. Li, and Z. Pan, “Toward green and soft: A 5G perspective,” *IEEE Communications Magazine*, vol. 52, no. 2, pp. 66–73, 2014.
- [28] P. Taylor, “Text-to-speech synthesis,” *Cambridge university press*, 2009.
- [29] R. Garg, P. Bhartia, I. J. Bahl, and A. Ittipiboon, “Microstrip antenna design handbook,” *Artech house*, 2001.
- [30] R. Bancroft, “Microstrip and printed antenna design,” *The Institution of Engineering and Technology*, 2009.

- [31] “Radar Basics - Patch Antennas,”
<https://www.radartutorial.eu/06.antennas/Microstrip%20Antenna.en.html>.
- [32] Y. Huang and K. Boyle, “Antennas: from theory to practice,” *John Wiley & Sons*, 2008.
- [33] C. A. Balanis, “Antenna Theory: Analysis and Design,” *John Wiley & Sons*, 2005.
- [34] H. Schantz, “Ultrawideband antennas,” *Artech House, Inc.*, 2005.
- [35] “Antenna Efficiency,” <http://www.antenna-theory.com/basics/efficiency.php>.
- [36] C. Ryan and L. Peters, “Evaluation of edge-diffracted fields including equivalent currents for the caustic regions,” *IEEE Transactions on Antennas and Propagation*, vol. 17, no. 3, pp. 292–299, 1969.
- [37] M. I. Skolnik, “Radar Handbook,” *McGraw-Hill Professional*, 1990.
- [38] A. K. Rastogi, M. Bano, and S. Sharma, “Design and Simulation Model for Compensated and Optimized T-junctions in Microstrip Line,” vol. 3, no. 12, pp. 5, 2014.
- [39] D. M. Pozar, “Microwave engineering,” *John Wiley & Sons*, 2009.